High energy resummation effects in heavy quarkonium production at LLA and beyond

Maxim Nefedov[1]
In collaboration with: Mathias Butenschoen, Chris Flett, Jean-Philippe Lansberg, Saad Nabeebaccus and Melih Ozcelik

"Next gen. pQCD for Hadron structure",
MITP, Mainz, October 29th., 2024

This project is supported by the European Commission's Marie Skłodowska-Curie action "RadCor4HEF", grant agreement No. 101065263

[1]Université Paris-Saclay, CNRS, IJCLab, Orsay, France

Outline

1. Overview: inclusive heavy quarkonium production physics, approaches and puzzles
2. Inclusive quarkonium production at high energy, curing the perturbative instability
3. Exclusive J/ψ photoproduction
4. Beyond DLA: NLO impact-factor for the forward η_c hadroproduction and comparisons with Collinear Factorisation at NLO

Overview: inclusive heavy-quarkonium production, approaches and puzzles

Motivations (I): understanding hadronisation

Description of production of any high-$p_T(\gg \Lambda_{\rm QCD})$ hadrons in QCD = (perturbative) production of quarks/gluons + *hadronisation.*

1. For light and heavy-light hadrons, hadronisation is studied phenomenologically:
   - Fragmantation Functions: based on factorisation theorems, fitted to describe data
   - Monte-Carlo models: hard to derive from QCD Lagrangian (string-based in Pythia, cluster hadronisation in Herwig,...)
2. Quarkonia – "Hydrogen atoms of QCD" ⇒ corrections to the "naive" quark model should be suppressed by powers of relative velocity (v) of heavy quarks in the bound state:

$$\begin{aligned} |J/\psi\rangle &= O(1)\left|c\bar{c}\left[{}^3S_1^{(1)}\right]\right\rangle + O(v)\left|c\bar{c}\left[{}^3P_J^{(8)}\right]+g\right\rangle \\ &+ O(v^2)\left|c\bar{c}\left[{}^1S_0^{(8)}\right]+g\right\rangle + O(v^2)\left|c\bar{c}\left[{}^3S_1^{(8)}\right]+gg\right\rangle + \ldots, \end{aligned}$$

3. ⇒ let's try to use understand production of quarkonia. **This understanding will be a small-v limit for any future theory of hadronisation!**

Motivations (II): quarkonia as tools

If hadronisation mechanism **was well understood,** *then quarkonium production would be:*

1. An excellent tool to study gluon content of a proton/nucleus:
   - Small (or negligible) “valence” c and b content – production predominantly through coupling to gluons at high energies
   - Clean experimental signatures for J/ψ, $\Upsilon(nS)$, ...
   - relatively small $M_{J/\psi} \simeq 3GeV$ – *access to very small* $x \sim Me^{-y}/\sqrt{s} \sim 10^{-4} - 10^{-6}$ at the LHC.
2. A tool to study double/multiple parton scattering: due to significant cross sections of multiple/associated production and lower p_T/scales in comparison to vector bosons/jets
3. A probe for QGP: melting/recombination/parton energy loss could be studied
4. ...

Physics case for quarkonium studies at the Electron Ion Collider

Daniël Boer[a,1], Chris A. Flett[b,1], Carlo Flore[b,c,d,1], Daniel Kikoła[e,1], Jean-Philippe Lansberg[b,1], Maxim Nefedov[b,1], Charlotte Van Hulse[b,f,1], Shohini Bhattacharya[g], Jelle Bor[a,b], Mathias Butenschoen[h], Federico Ceccopieri[b,i], Longjie Chen[j,k], Vincent Cheung[l], Umberto D’Alesio[d], Miguel Echevarria[m], Yoshitaka Hatta[g,n], Charles E. Hyde[o], Raj Kishore[m,p], Leszek Kosarzewski[q], Cédric Lorcé[r], Wenliang Li[p,s], Xuan Li[t], Luca Maxia[a,d], Andreas Metz[u], Asmita Mukherjee[v], Carlos Muñoz Camacho[b], Francesco Murgia[d], Pawel Nadel-Turonski[r,w], Cristian Pisano[d], Jian-Wei Qiu[x], Sangem Rajesh[y], Matteo Rinaldi[z], Jennifer Rittenhouse West[aa,ab], Vladimir Saleev[ac], Nathaly Santiesteban[ad], Chalis Setyadi[a,ae], Pieter Taels[af], Zhoudunmin Tu[g], Ivan Vitev[t], Ramona Vogt[l,ag], Kazuhiro Watanabe[ah,ai], Xiaojun Yao[aj,ak], Yelyzaveta Yedelkina[b,al], Shinsuke Yoshida[j,k]

Quarkonium production models

Unfortunately no existing model can describe all data on inclusive quarkonium hadro/photo/electro/e^+e^- production and polarisation observables.

Old ideas:

1. Colour Singlet Model: only **colour-singlet** $Q\bar{Q}$ pairs with the same orbital momentum/spin as corresponding potential-model state hadronise to the quarkonium.
2. NRQCD factorisation: based on the hierarchy of different colour/orbital momentum/spin states of the $Q\bar{Q}$-pair in the v-expansion for the quarkonium state
3. (Improved) Colour Evaporation Model assumes "democracy" of colour/orbital momentum/spin states of the $Q\bar{Q}$-pair

New ideas: Potential NRQCD, Soft-gluon factorisation, Shape-functions, ...

Motivation for new ideas:

- reduction of the numeber of free parameters
- improvement of perturbative convergence
- phenomenological problems

Quarkonium in the potential model

Cornell potential:

$$V(r) = -C_F \frac{\alpha_s(1/r)}{r} + \sigma r,$$

neglect linear part, because quarkonium is "small" (~ 0.3 fm) $\to$ Coulomb wavefunction (for effective mass $\frac{m_1 m_2}{m_1+m_2} = \frac{m_Q}{2}$):

$$R(r) = \frac{\sqrt{m_Q^3 \alpha_s^3 C_F^3}}{2} e^{-\frac{\alpha_s C_F}{2} m_Q r}$$

$$\langle v^2 \rangle = \frac{C_F^2 \alpha_s^2}{2}, \langle r \rangle = \frac{3}{2C_F} \frac{1}{m_Q v}$$

$$\Rightarrow \boxed{\alpha_s^2(m_Q v) \simeq v^2}$$

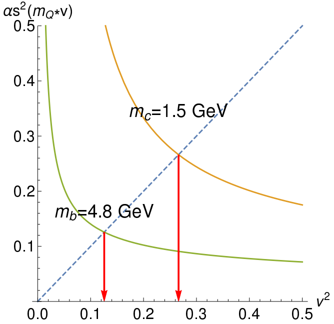

Non-relativistic QCD

The velocity-expansion for quarkonium eigenstate is a copy of corresponding arguments from atomic physics:

$$\begin{aligned} |J/\psi\rangle &= O(1)\left|c\bar{c}\left[{}^3S_1^{(1)}\right]\right\rangle + O(v)\left|c\bar{c}\left[{}^3P_J^{(8)}\right]+g\right\rangle \\ &+ O(v^2)\left|c\bar{c}\left[{}^1S_0^{(8)}\right]+g\right\rangle + O(v^2)\left|c\bar{c}\left[{}^3S_1^{(8)}\right]+gg\right\rangle + \ldots, \end{aligned}$$

for validity of this arguments, we should work in *non-relativistic EFT*, dynamics of which conserves number of heavy quarks. In such EFT, $Q\bar{Q}$-pair is produced in a point, by local operator:

$$\mathcal{A}_{\mathrm{NRQCD}} = \langle J/\psi + X|\, \chi^\dagger(0)\kappa_n\psi(0)\,|0\rangle\,,$$

Different operators "couple" to different Fock states:

$$\chi^\dagger(0)\psi(0) \leftrightarrow \left|c\bar{c}\left[{}^1S_0^{(1)}\right]\right\rangle,\ \chi^\dagger(0)\sigma_i\psi(0) \leftrightarrow \left|c\bar{c}\left[{}^3S_1^{(1)}\right]\right\rangle,$$
$$\chi^\dagger(0)\sigma_i T^a\psi(0) \leftrightarrow \left|c\bar{c}\left[{}^3S_1^{(8)}\right]\right\rangle,\ \chi^\dagger(0)D_i\psi(0) \leftrightarrow \left|c\bar{c}\left[{}^1P_1^{(8)}\right]\right\rangle, \ldots$$

squared NRQCD amplitude (=LDME):

$$\sum_X |\mathcal{A}|^2 = \langle 0|\underbrace{\psi^\dagger\kappa_n^\dagger\chi a^\dagger_{J/\psi}a_{J/\psi}\chi^\dagger\kappa_n\psi}_{\mathcal{O}_n^{J/\psi}}|0\rangle = \left\langle \mathcal{O}_n^{J/\psi}\right\rangle,$$

Velocity-scaling of LDMEs follows from velocity-scaling of corresponding Fock states and of operators $\chi^\dagger \kappa_n \psi$:

	${}^1S_0^{(1)}$	${}^3S_1^{(1)}$	${}^1S_0^{(8)}$	${}^3S_1^{(8)}$	${}^1P_1^{(1)}$	${}^3P_0^{(1)}$	${}^3P_1^{(1)}$	${}^3P_2^{(1)}$	${}^1P_1^{(8)}$	${}^3P_0^{(8)}$	${}^3P_1^{(8)}$	${}^3P_2^{(8)}$
η_c	1		v^4	v^4					v^4			
J/ψ		1	v^4	v^4						v^4	v^4	v^4
h_c			v^2		v^2							
χ_{c0}				v^2		v^2						
χ_{c1}				v^2			v^2					
χ_{c2}				v^2				v^2				

Note that:

- Colour-singlet LDMEs are LO in v for S-wave states $\Rightarrow$ *Colour-Singlet Model*
- For P-wave states the CS and CO LDMEs are of the same order $\Rightarrow$ *mixing*
- Connection between LDMEs for η_c and J/ψ through *Heavy-Quark Spin Symmetry*

Matching procedure between QCD and NRQCD:

$$v \ll 1 : \mathcal{A}_{\rm QCD}(gg \to Y_{Q\bar{Q}(v)}) = \sum_n f_n \left\langle Y_{Q\bar{Q}(v)} \right| \chi^\dagger(0)\kappa_n\psi(0) \left|0\right\rangle + O(v^{\#}),$$

$\Rightarrow$ NRQCD factorization formula ("theorem") [Bodwin, Braaten, Lepage 95'] :

$$\sigma(gg \to \mathcal{H} + X) = \sum_n \sigma(gg \to Q\bar{Q}[n] + X) \left\langle \mathcal{O}_n^{\mathcal{H}} \right\rangle .$$

NRQCD factorisation: p_T-behaviour in pp

$$\frac{d\sigma}{dp_T^2}(pp \to \mathcal{H} + X) = \sum_n \frac{d\sigma}{dp_T^2}(pp \to Q\bar{Q}[n] + X) \left\langle \mathcal{O}_n^{\mathcal{H}} \right\rangle .$$

NLO, plot from hep-ph/1403.3970 :

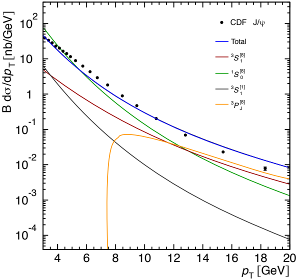

At **LO**:

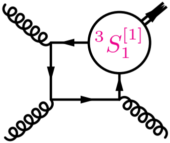

$\sim p_T^{-8}$

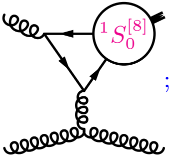

;

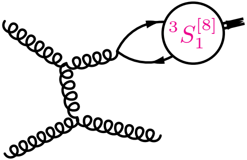

$\sim p_T^{-4}$

Free parameters:

- For S-wave ($S = 1$) state (J/ψ, $\psi(2S)$, $\Upsilon(nS)$): $^3S_1^{[1]}$ – known from potential model, $^1S_0^{[8]}$, $^3S_1^{[8]}$, $^3P_0^{[8]}$ – are fitted
- For P-wave ($S = 1$) state (χ_{cJ}, χ_{bJ}): $^3P_0^{[1]}$ – known from potential model, $^3S_1^{[8]}$ is fitted.
- LDMEs for $S = 0$ states ($\eta_{c,b}$, $h_{c,b}$) are obtained from $S = 1$ ones through the HQSS

Potential NRQCD: more relations between LDMEs

The NRQCD logic can be pushed even further by assuming that $mv^2 \ll mv$ [Brambilla et.al., '22] . **At LO in** v:

Prompt cross section ratios:

$$\boxed{\langle \mathcal{O}^{\mathcal{H}}(^3S_1^{[1]})\rangle = \frac{3N_c}{2\pi}|R_{\mathcal{H}}(0)|^2,}$$

$$\langle \mathcal{O}^{\mathcal{H}}(^3P_J^{[8]})\rangle = \frac{2J+1}{18N_c}\frac{3|R_{\mathcal{H}}(0)|^2}{4\pi}\mathcal{E}_{00},$$

$$\langle \mathcal{O}^{\mathcal{H}}(^1S_0^{[8]})\rangle = \frac{1}{6N_c m^2}\frac{3|R_{\mathcal{H}}(0)|^2}{4\pi}c_F^2\mathcal{B}_{00},$$

$$\langle \mathcal{O}^{\mathcal{H}}(^3S_1^{[8]})\rangle = \frac{1}{2N_c m^2}\frac{3|R_{\mathcal{H}}(0)|^2}{4\pi}\mathcal{E}_{10;10},$$

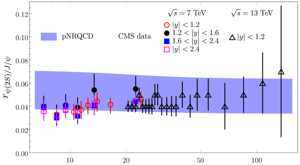

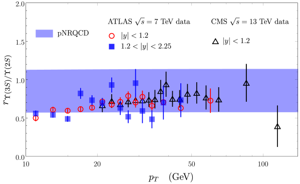

where $|R_{\mathcal{H}}(0)|^2$ – radial wave function at the origin from **potential model** for the quarkonium $\mathcal{H}$, and $\mathcal{E}_{00}$, $\mathcal{B}_{00}$, $\mathcal{E}_{10;10}$ – chromo electric/magnetic field correlators over QCD vacuum (i.e. **independent on** $\mathcal{H}$ up to RG running $m_c \to m_b$).

NRQCD factorisation: what does work?

- *Un-polarized* p_T distributions of J/ψ, χ_{cJ} in hadro- and photoproduction, as well as e^+e^- data can be described. The same is true for $\Upsilon(nS)$, $\chi_{bJ}(nS)$.
- Solves the problem of non-cancelling IR divergence at NLO in CSM for P-wave states production and decay through mixing with ${}^3S_1^{(8)}$ or ${}^1S_0^{(8)}$ states at $O(v^2)$.
- Covers the gap between CSM (@LO and NLO) and data at high-p_T in hadroproduction, due to contribution of CO states. If NNLO corrections in CS are as large as needed to close this gap, then perturbative expansion is just useless and we should stop doing quarkonia.

NLO NRQCD, [Butenschön, Kniehl, '11]

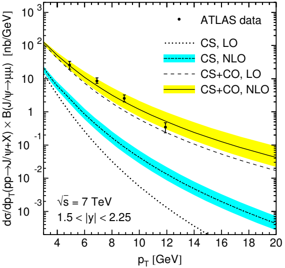

NLO and NNLO* CSM [Lansberg '11]

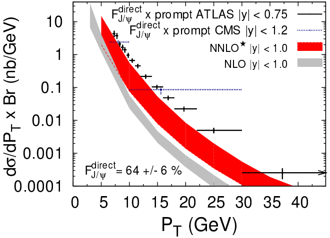

Problems: Polarisation

LDME fit	J/ψ hadropr.	J/ψ photopr.	J/ψ polar.	η_c hadropr.
Butenschön et al.	✓($p_T > 3$ GeV)	✓	✗	✗
Chao et al. + η_c	✓($p_T > 6.5$ GeV)	✗	✓	✓
Zhang et al.	✓($p_T > 6.5$ GeV)	✗	✓	✓
Gong et al.	✓($p_T > 7$ GeV)	✗	✓	✗
Chao et al.	✓($p_T > 7$ GeV)	✗	✓	✗
Bodwin et al.	✓($p_T > 10$ GeV)	✗	✓	✗

Global fit [Butenschön, Kniehl, '12]

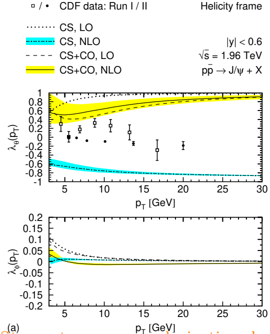

Strong transverse polarisation due to ${}^3S_1^{[8]}$ and ${}^3P_J^{[8]}$ states at high p_T

E.g. hadroproduction dominated fit

[Chao et.al., '14]

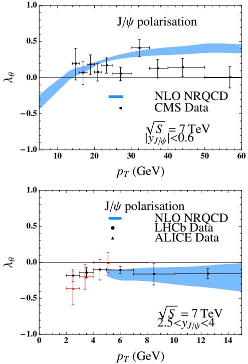

Problems: HQSS and photoproduction

LDME fit	J/ψ hadropr.	J/ψ photopr.	J/ψ polar.	η_c hadropr.
Butenschön et al.	✓($p_T > 3$ GeV)	✓	✗	✗
Chao et al. + η_c	✓($p_T > 6.5$ GeV)	✗	✓	✓
Zhang et al.	✓($p_T > 6.5$ GeV)	✗	✓	✓
Gong et al.	✓($p_T > 7$ GeV)	✗	✓	✗
Chao et al.	✓($p_T > 7$ GeV)	✗	✓	✗
Bodwin et al.	✓($p_T > 10$ GeV)	✗	✓	✗

Global fit [Butenschön, Kniehl, '12]

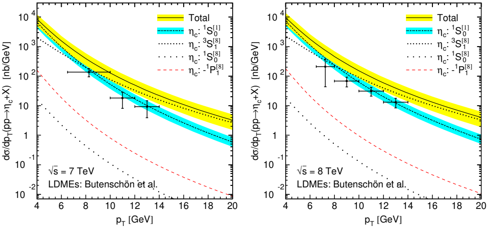

J/ψ-photoproduction at the EIC vs $z = (p_{J/\psi}P)/(qP)$, using NLO calculation

data by M. Butenschön

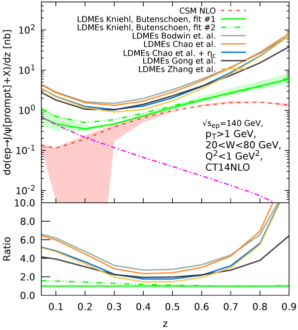

Slides from M. Butenschön at **QaT-2021**:

3.2 Butenschön et al. LDMEs

12/18

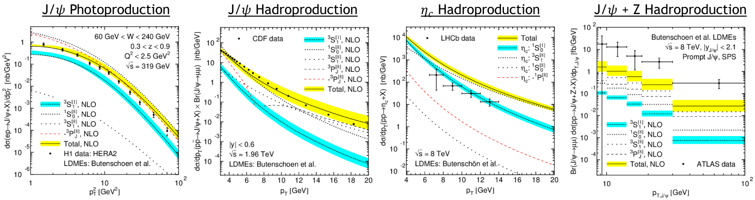

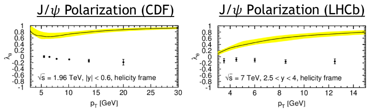

- Fit to 194 data points of J/ψ photo- and hadro-production, $\gamma\gamma$- and e^+e^- scattering
- $<O^{J/\psi}$(1S08)>=4.97±0.44, $<O^{J/\psi}$(3S18)>=0.22±0.06, $<O^{J/\psi}$(3P08)>=-1.61±0.20 [in 10^{-2} GeV^3 or 10^{-2} GeV^5]
- Ref.: [MB, Kniehl, PRD 84, 051501 (2011)]

- Data fitted to is described within scale uncertainties, other observables not.

Slides from M. Butenschön at **QaT-2021**:

3.4 Chao et al. LDMEs

14/18

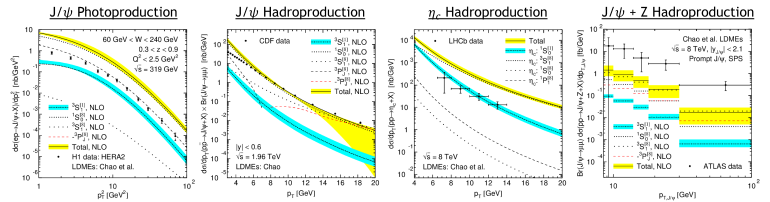

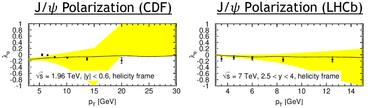

- Fit to CDF J/ψ yield and polarization with $p_T > 7$ GeV.
- $<O^{J/\psi}$(1S08)>=8.9 $\pm$0.98, $<O^{J/\psi}$(3S18)>=0.30 $\pm$0.12, $<O^{J/\psi}$(3P08)>=1.26 $\pm$0.47 [in 10^{-2} GeV^3 or 10^{-2} GeV^5]
- Ref.: [Chao, Ma, Shao, Wang, Zhang, PRL 108, 242004 (2012)]

- Data fitted to is described, other observables not.

Slides from M. Butenschön at **QaT-2021**:

3.5 Chao et al. LDMEs: With η_c

15/18

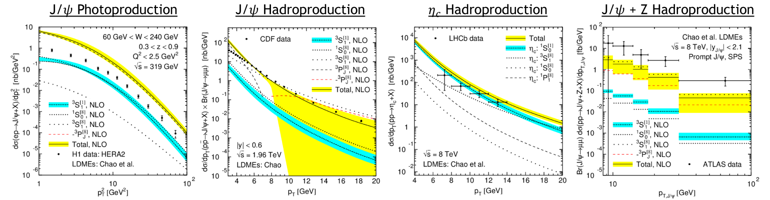

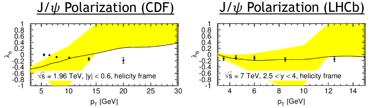

- Fit to CDF J/ψ yield $p_T > 7$ GeV (contraining two linear combinations M_0 and M_1) plus the LHCb η_c production data (constraining $<O^{J/\psi}$(1S08)>)
- $<O^{J/\psi}$(1S08)>=0.73 $\pm$0.73, $<O^{J/\psi}$(3S18)>=1.0 $\pm$0.3, $<O^{J/\psi}$(3P08)>=3.8 $\pm$1.1 [in 10^{-2} GeV^3 or 10^{-2} GeV^5]
- Ref.: [Han, Ma, Meng, Shao, Chao, PRL 114 (2015) 092005]

- Nontrivial: Largely unpolarized J/ψ compatible with data (although tensions to CDF data). But: J/ψ hadroproduction $p_T < 7$ GeV, J/ψ photo- and J/$\psi + Z$ production not described.

Slides from M. Butenschön at **QaT-2021**:

3.7 Bodwin et al. LDMEs

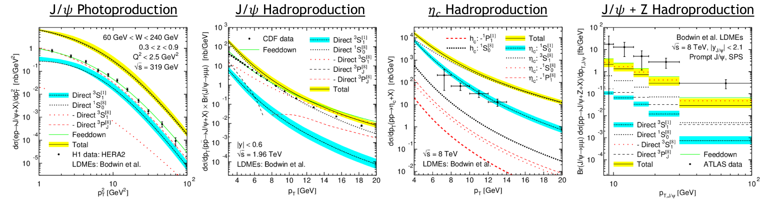

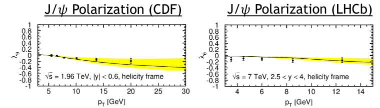

- Fit to $J/\psi, \psi(2S)$, χ_{cJ} hadroproduction yield with $p_T > 3m_H$.
- Includes resummed FFs (we don't here → 2nd plot: small deviations)
- $\langle O^{J/\psi}(1S08)\rangle$=11±1.4, $\langle O^{J/\psi}(3S18)\rangle$=-0.71±0.36, $\langle O^{J/\psi}(3P08)\rangle$=-0.70±0.34, $\langle O^{\psi(2S)}(1S08)\rangle$=3.14±0.79, $\langle O^{\psi(2S)}(3S18)\rangle$=-0.16 ±0.28, $\langle O^{\psi(2S)}(3P08)\rangle$=-0.26±0.27, $\langle O^{\chi_{c0}}(3P01)\rangle$=7.94 ±2.43, $\langle O^{\chi_{c0}}(3S18)\rangle$=0.57±0.13 [$10^{-2}$ GeV$^{3 \text{ or } 5}$]
- Ref.: [Bodwin, Chao, Chung, Kim, Lee, Ma, PRD 93, 034041 (2016)]

- Nontrivial outcome: Unpolarized J/ψ compatible with data.
  But: Small- and mid-p_T J/ψ hadro-; J/ψ photo-, η_c and $J/\psi + Z$ production not described.

z-differential J/ψ photoproduction

Variable $z = \frac{p_{J/\psi} \cdot P}{q \cdot P}$.

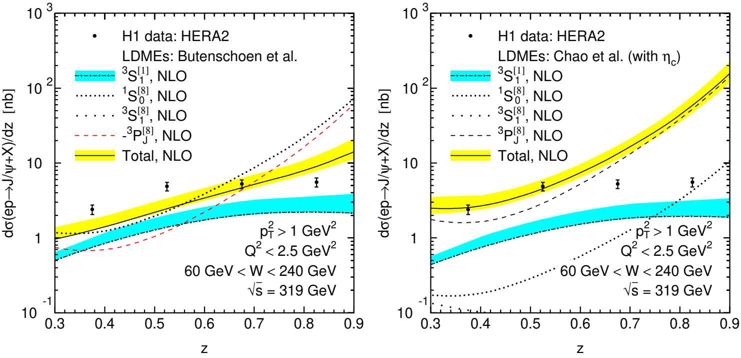

The "hadroproduction-dominated" fits actually describe the data for $z < 0.6$!

Inclusive heavy quarkonium production at moderate p_T

Quarkonium production p_T spectra at $p_T \gtrsim M$ are not described by collinear factorisation computations at NLO. Example: η_c production at LHCb [LHCb, '24] (left panel $d\sigma/dp_T$, right panel: ratio to J/ψ):

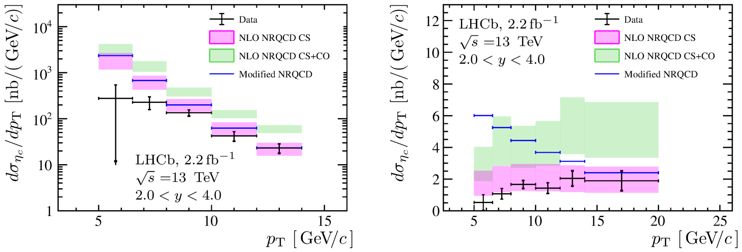

- NLO CF overshoots the data for $5 < p_T < 8$ GeV: nothing to do with TMD/Sudakov logs ($\ln p_T/M$) which contribute only at $p_T \ll M \simeq 3$ GeV
- Physical shape of the p_T-spectrum is reproduced in k_T-factorisation [Kniehl, Vasin, Saleev '06;...;MN,Saleev,Shipilova '12;...] and Saturation/CGC calculations [Kang, Ma, Venugopalan '13; ... Mantysaari *et al.* '24] **at LO in** α_s

Intermediate conclusions

- NRQCD factorisation remains the "standard theory" of quarkonium production, pNRQCD factorisation or introduction of shape functions (talk of Luca Maxia last week) are based on the v^2-expansion
- The main phenomenological problem of NRQCD-factorisation is the inconsistency between hadroproduction and photoproduction at $z \to 1$.
- The problems with p_T-spectrum at $p_T \lesssim M$ and with p_T-integrated cross sections can be resolved within perturbation theory (this talk)

I. Inclusive quarkonium production at high energy

In collaboration with Jean-Philippe Lansberg and Melih Ozcelik.
Based on JHEP **05** (2022) 083; Eur.Phys.J.C 84 (2024) 4, 351 and ongoing work

Perturbative instability of quarkonium total cross sections

Inclusive η_c-hadroproduction (CSM)

[Mangano *et.al.*, '97, ..., Lansberg, Ozcelik, '20]

$$p+p \to c\bar{c}\left[{}^1S_0^{[1]}\right]+X,\ \text{LO: } g(p_1)+g(p_2) \to c\bar{c}\left[{}^1S_0^{[1]}\right],$$

$$\sigma(\sqrt{s_{pp}}) = f_i(x_1,\mu_F) \otimes f_j(x_2,\mu_F) \otimes \hat{\sigma}(z),$$

where $z = \frac{M^2}{\hat{s}}$ with $\hat{s} = (p_1+p_2)^2$.

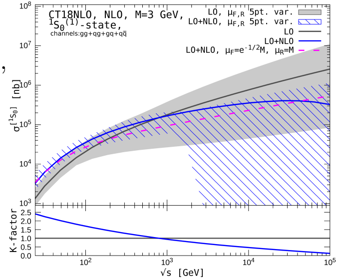

Inclusive J/ψ-photoproduction (CSM)

[Krämer, '96, ...,Colpani Serri *et.al*, '21]

$$\gamma+p \to c\bar{c}\left[{}^3S_1^{[1]}\right]+X,\ \text{LO: } \gamma(q)+g(p_1) \to c\bar{c}\left[{}^3S_1^{[1]}\right]+g,$$

$$\sigma(\sqrt{s_{\gamma p}}) = f_i(x_1,\mu_F) \otimes \hat{\sigma}(\eta),$$

where $\eta = \frac{\hat{s}-M^2}{M^2}$ with $\hat{s} = (q+p_1)^2$, $z = \frac{pP}{qP}$.

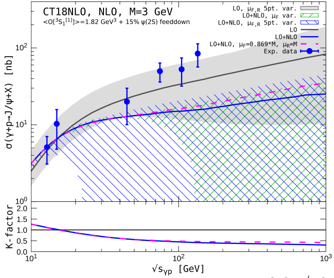

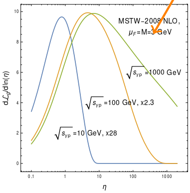

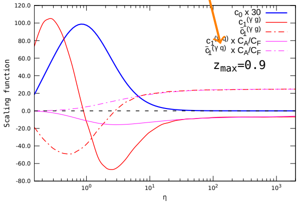

Partonic high-energy logarithms

$$\sigma(x) \propto \int_0^1 \frac{dz}{z} C(z) \tilde{f}_g(x/z, \mu^2),$$

where $\tilde{f}_g(x, \mu^2) = x f_g(x, \mu^2)$.
Suppose for $z \ll 1$: $C(z) \sim \alpha_s^n(\mu) \ln^{n-1}(1/z)$ and $\tilde{f}_g(x, \mu^2) \sim x^{-\alpha(\mu)}$. Then for $x \ll 1$:

$$\sigma(x) \sim x^{-\alpha} \left(\frac{\alpha_s(\mu)}{\alpha(\mu)} \right)^n,$$

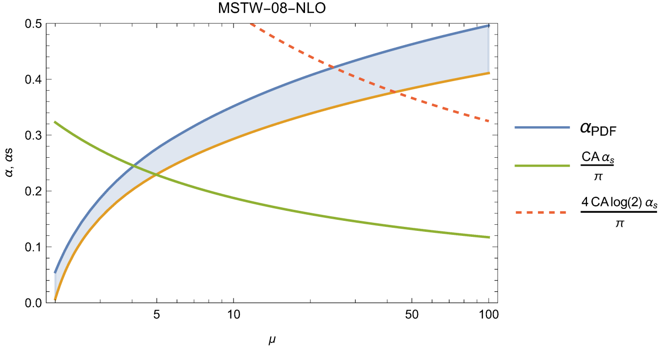

High-Energy Factorization (J/ψ photoproduction)

The **LLA** ($\sum_n \alpha_s^n \ln^{n-1}$) formalism [Collins, Ellis, '91; Catani, Ciafaloni, Hautmann, '91,'94]

Physical picture in the **LLA** for photoproduction:

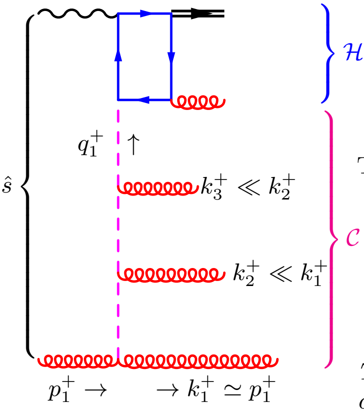

The LLA in $\ln \frac{1}{\xi} = \ln \frac{p_1^+}{q_1^+} \sim \ln(1+\eta)$:

$$\hat{\sigma}_{\mathrm{HEF}}^{\ln(1/\xi)}(\eta) \propto \int\limits_{1/z}^{1+\eta} \frac{dy}{y} \int\limits_{0}^{\infty} d\mathbf{q}_{T1}^2 \mathcal{C}\left(\frac{y}{1+\eta}, \mathbf{q}_{T1}^2, \mu_F, \mu_R\right) \mathcal{H}(y, \mathbf{q}_{T1}^2),$$

The **strict LLA** in $\ln(1+\eta) = \ln \frac{\hat{s}}{M^2}$:

$$\hat{\sigma}_{\mathrm{HEF}}^{\ln(1+\eta)}(\eta) \propto \int\limits_{0}^{\infty} d\mathbf{q}_{T1}^2 \mathcal{C}\left(\frac{1}{1+\eta}, \mathbf{q}_{T1}^2, \mu_F, \mu_R\right) \int\limits_{1/z}^{\infty} \frac{dy}{y} \mathcal{H}(y, \mathbf{q}_{T1}^2).$$

The LLA($\ln(1/\xi)$) contains some (N..)NLLA contributions relative to the LLA($\ln(1+\eta)$).

The coefficient function $\mathcal{H}$ has been calculated at LO [Kniehl, Vasin, Saleev, '06] and decreases as $1/y^2$ for $y \gg 1$.

High-Energy Factorization (η_c hadroproduction)

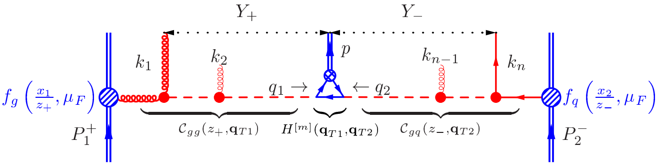

Small parameter: $z = \frac{M^2}{\hat{s}}$, LLA in $\alpha_s^n \ln^{n-1} \frac{1}{z}$:

$$\hat{\sigma}_{ij}^{[m],\text{ HEF}}(z, \mu_F, \mu_R) = \int\limits_{-\infty}^{\infty} d\eta \int\limits_{0}^{\infty} d\mathbf{q}_{T1}^2 d\mathbf{q}_{T2}^2 \, \mathcal{C}_{gi}\left(\frac{M_T}{M}\sqrt{z}e^{\eta}, \mathbf{q}_{T1}^2, \mu_F, \mu_R\right)$$

$$\times \mathcal{C}_{gj}\left(\frac{M_T}{M}\sqrt{z}e^{-\eta}, \mathbf{q}_{T2}^2, \mu_F, \mu_R\right) \int\limits_{0}^{2\pi} \frac{d\phi}{2} \frac{H^{[m]}(\mathbf{q}_{T1}^2, \mathbf{q}_{T2}^2, \phi)}{M_T^4}$$

The coefficient functions $H^{[m]}$ are known at LO in α_s [Hagler *et.al*, 2000; Kniehl, Vasin, Saleev 2006] for $m = {}^1S_0^{(1,8)}, {}^3P_J^{(1,8)}, {}^3S_1^{(8)}$.
The $H^{[m]}$ is a tree-level "squared matrix element" of the $2 \to 1$-type process:

$$R_+(\mathbf{q}_{T1}, q_1^+) + R_-(\mathbf{q}_{T2}, q_2^-) \to c\bar{c}[m].$$

LLA evolution w.r.t. $\ln 1/\xi$

In the LL($\ln 1/\xi$)-approximation, the $Y = \ln 1/\xi$-evolution equation for *collinearly un-subtracted* $\tilde{\mathcal{C}}$-factor has the form:

$$\tilde{\mathcal{C}}(\xi, \mathbf{q}_T) = \delta(1-\xi)\delta(\mathbf{q}_T^2) + \hat{\alpha}_s \int\limits_{\xi}^{1} \frac{dz}{z} \int d^{2-2\epsilon}\mathbf{k}_T K(\mathbf{k}_T^2, \mathbf{q}_T^2) \tilde{\mathcal{C}}\left(\frac{\xi}{z}, \mathbf{q}_T - \mathbf{k}_T\right)$$

with $\hat{\alpha}_s = \alpha_s C_A/\pi$ and

$$K(\mathbf{k}_T^2, \mathbf{q}_T^2) = \frac{1}{\pi(2\pi)^{-2\epsilon}\mathbf{k}_T^2} + \delta^{(2-2\epsilon)}(\mathbf{k}_T)\ 2\omega_g(\mathbf{q}_T^2),$$

where $\omega_g(\mathbf{q}_T^2)$ – 1-loop Regge trajectory of a gluon. It is convenient to go from $(z, \mathbf{q}_T)$-space to $(N, \mathbf{x}_T)$-space:

$$\tilde{\mathcal{C}}(N, \mathbf{x}_T) = \int d^{2-2\epsilon}\mathbf{q}_T\ e^{i\mathbf{x}_T\mathbf{q}_T} \int\limits_0^1 dx\ x^{N-1}\ \tilde{\mathcal{C}}(x, \mathbf{q}_T),$$

because:

- Mellin convolutions over z turn into products: $\int \frac{dz}{z} \to \frac{1}{N}$
- Large logs map to poles at $N = 0$: $\boxed{\alpha_s^{k+1} \ln^{k} \frac{1}{\xi} \to \frac{\alpha_s^{k+1}}{N^{k+1}}}$
- All *collinear divergences* are contained inside $\mathcal{C}$ in $\mathbf{x}_T$-space.

Exact LL solution and the DLA

In $(N, \mathbf{q}_T)$-space, subtracted $\mathcal{C}$, which resums all terms $\propto (\hat{\alpha}_s/N)^n$ (complete LLA) has the form [Collins, Ellis, '91; Catani, Ciafaloni, Hautmann, '91,'94]:

$$\mathcal{C}(N, \mathbf{q}_T, \mu_F) = R(\gamma_{gg}(N,\alpha_s))\frac{\gamma_{gg}(N,\alpha_s)}{\mathbf{q}_T^2}\left(\frac{\mathbf{q}_T^2}{\mu_F^2}\right)^{\gamma_{gg}(N,\alpha_s)},$$

where $\gamma_{gg}(N,\alpha_s)$ is the solution of [Jaroszewicz, '82]:

$$\frac{\hat{\alpha}_s}{N}\chi(\gamma_{gg}(N,\alpha_s)) = 1, \text{ with } \chi(\gamma) = 2\psi(1) - \psi(\gamma) - \psi(1-\gamma),$$

where $\psi(\gamma) = d\ln\Gamma(\gamma)/d\gamma$ – Euler's ψ-function. The first few terms:

$$\gamma_{gg}(N,\alpha_s) = \underbrace{\underbrace{\frac{\hat{\alpha}_s}{N}}_{\text{DLA [Blümlein, '95]}} + 2\zeta(3)\frac{\hat{\alpha}_s^4}{N^4} + 2\zeta(5)\frac{\hat{\alpha}_s^6}{N^6} + \ldots}_{\text{LLA}}$$

$\frac{\hat{\alpha}_s}{N} \leftrightarrow P_{gg}(z\to 0) = \frac{2C_A}{z} + \ldots$

The function $R(\gamma)$ is

$$R(\gamma_{gg}(N,\alpha_s)) = 1 + O(\alpha_s^3).$$

Fixed-order asymptotics from HEF

When expanded up to $O(\alpha_s)$ the HEF resummation should predict the $\hat{s} \gg M^2$ asymptotics of the CF coefficient function $\hat{\sigma}$

For the $g + g \to c\bar{c}\left[{}^1S_0^{(1)}, {}^3P_0^{(1)}, {}^3P_2^{(1)}\right]$ the NLO and NNLO($\alpha_s^2 \ln(1/z)$) terms in $\hat{\sigma}$ are predicted [M.N., Lansberg, Ozcelik '22]:

State	$A_0^{[m]}$	$A_1^{[m]}$	$A_2^{[m]}$	$B_2^{[m]}$
${}^1S_0$	1	-1	$\frac{\pi^2}{6}$	$\frac{\pi^2}{6}$
${}^3S_1$	0	1	0	$\frac{\pi^2}{6}$
${}^3P_0$	1	$-\frac{43}{27}$	$\frac{\pi^2}{6} + \frac{2}{3}$	$\frac{\pi^2}{6} + \frac{40}{27}$
${}^3P_1$	0	$\frac{5}{54}$	$-\frac{1}{9}$	$-\frac{2}{9}$
${}^3P_2$	1	$-\frac{53}{36}$	$\frac{\pi^2}{6} + \frac{1}{2}$	$\frac{\pi^2}{6} + \frac{11}{9}$

$$\hat{\sigma}_{gg}^{[m]}(z \to 0) = \sigma_{\rm LO}^{[m]} \left\{ A_0^{[m]} \delta(1-z) + \frac{\alpha_s}{\pi} 2C_A \left[A_1^{[m]} + A_0^{[m]} \ln \frac{M^2}{\mu_F^2} \right] + \left(\frac{\alpha_s}{\pi}\right)^2 \ln\frac{1}{z} \cdot C_A^2 \left[2A_2^{[m]} + B_2^{[m]} + 4A_1^{[m]} \ln \frac{M^2}{\mu_F^2} + 2A_0^{[m]} \ln^2 \frac{M^2}{\mu_F^2} \right] + O(\alpha_s^3) \right\},$$

For the $\gamma + g \to c\bar{c}\left[{}^3S_1^{(1)}\right] + g$ we have computed $\eta \to \infty$ limit of the z and $\rho = \mathbf{p}_T^2/M^2$-differential NLO "scaling functions" in closed analytic form,

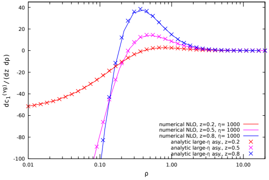

and obtained numerical results for NNLO "scaling function" c_2 in front of $\alpha_s \ln(1+\eta)$.

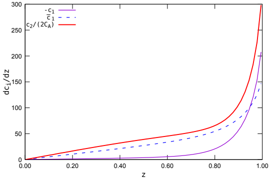

Inverse Error Weighting (InEW) matching

Development of an idea from [Echevarria *et al.*, 18'] :

$$\hat{\sigma}(\eta) = w_{\rm CF}(\eta)\hat{\sigma}_{\rm CF}(\eta) + (1 - w_{\rm CF}(\eta))\hat{\sigma}_{\rm HEF}(\eta),$$

the weights are determined through the estimates of "errors":

$$w_{\rm CF}(\eta) = \frac{\Delta\hat{\sigma}_{\rm CF}^{-2}(\eta)}{\Delta\hat{\sigma}_{\rm CF}^{-2}(\eta) + \Delta\hat{\sigma}_{\rm HEF}^{-2}(\eta)}, \quad w_{\rm HEF}(\eta) = 1 - w_{\rm CF}(\eta).$$

- $\Delta\hat{\sigma}_{\rm CF}(\eta)$ is due to **missing higher orders and large logarithms,** it can be estimated from the α_s expansion of $\hat{\sigma}_{\rm HEF}(\eta)$.
- $\Delta\hat{\sigma}_{\rm HEF}(\eta)$ is (mostly) due to **missing power corrections in** $1/\eta$: $\Delta\hat{\sigma}_{\rm HEF}(\eta) \sim A\eta^{-\alpha_{\rm HEF}}$. We determine A and $\alpha_{\rm HEF}$ from behaviour of $\hat{\sigma}_{\rm CF}(\eta) - \hat{\sigma}_{\rm CF}(\infty)$ at $\eta \gg 1$.

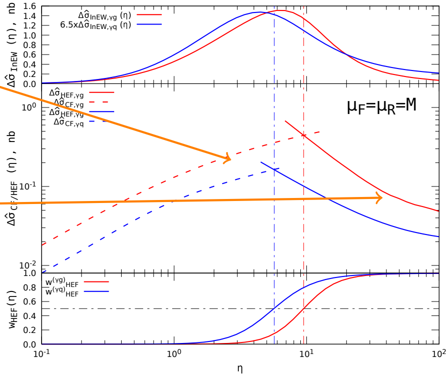

Matching with NLO

The HEF is valid in the **leading-power** in $M^2/\hat{s}$, so for $\hat{s} \sim M^2$ we match it with NLO CF by the *Inverse-Error Weighting Method* [Echevarria *et.al.*, 18'].

η_c**-hadroproduction**,
$z = M^2/\hat{s}$:

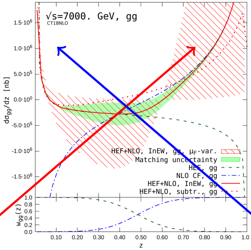

NLO **HEF**

J/ψ**-photoproduction**,
$\eta = (\hat{s} - M^2)/M^2$:

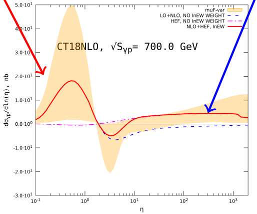

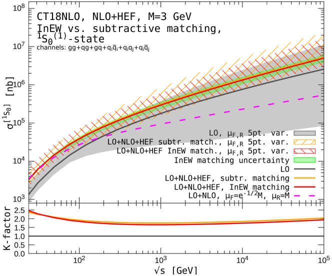

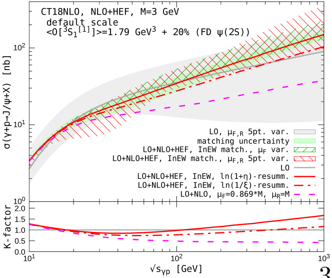

Vector quarkonium photoproduction: dynamical scale

Matched results for J/ψ photoproduction can be further improved by noticing that in the LO process:

$$\gamma(q) + g(p_1) \to Q\bar{Q}\left[{}^3S_1^{[1]}\right] + g,$$

the emitted gluon can not be soft, so that $\langle \hat{s} \rangle_{\rm LO}$ (~ 25 GeV^2 at high $\sqrt{s_{\gamma p}}$ for J/ψ) rather than M^2 can be taken as a default value of μ_F^2 and μ_R^2:

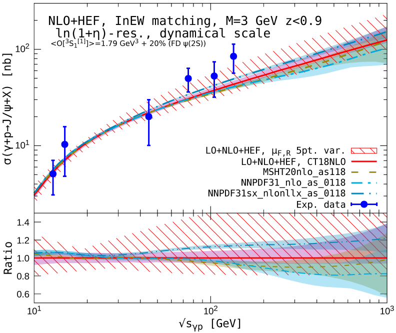

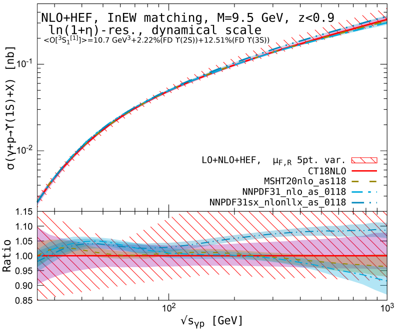

II. Exclusive J/ψ photoproduction at high energy

In collaboration with
Jean-Philippe Lansberg, Saad Nabeebaccus, Chris Flett,
Jakub Wagner(NCBJ, Warsaw) and Pawel Schnaider(NCBJ, Warsaw).

Exclusive photoproduction of vector quarkonia

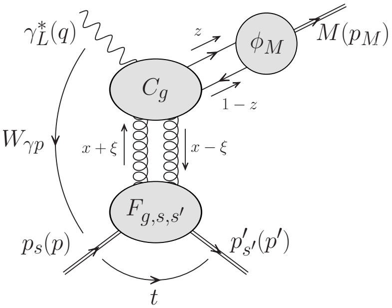

+ similar diagram with quark GPDs, starting from NLO.

- Hard exclusive reaction, similar to DVMP, but not "deeply virtual" ($q^2 \simeq 0$, $\perp$ photon). The quarkonium (J/ψ, Υ) mass $M_Q^2 \gg \Lambda_{\rm QCD}^2$ provides the hard scale
- Experimental data on $\sigma(W_{\gamma p})$ and $d\sigma/dt$ are available from *ep*-collisions (JLAB, HERA, COMPASS) and UPCs (ALICE, CMS, LHCb)
- Collinear Factorisation(CF) is not proven to all orders for the case when $q^2 \simeq 0$, but **complete** NLO computation [Ivanov, Schaefer, Szymanowsky, Krasnikov, 2004] in CF was done and it formally works.

Quarkonium is treated **non-relativistically**, either using $\phi(z, k_T)$ obtained from Schrödinger wavefunction (only at LO and usually in the high-energy regime) or even resorting to the "static" approximation $\phi(z) \propto R(0)\delta(z - 1/2)$, which corresponds to the strict LO in relative velocity of $Q\bar{Q}$ in the bound state (v^2).

Collinear factorisation

$$\mathcal{A} = -(\varepsilon_\mu^{*(\mathcal{Q})}\varepsilon_\nu^{(\gamma)} g_\perp^{\mu\nu}) \sum_{i=q,g} \int_{-1}^{1} \frac{dx}{x^{1+\delta_{ig}}} C_i\,(x,\xi)\,F_i(x,\xi,t,\mu_F),$$

CF coefficient function: $C_i = C_i^{(0)} + (\alpha_s(\mu_R)/\pi)C_i^{(1)} + \ldots$, with LO:

$$C_g^{(0)}\,(x,\xi) = \frac{x^2 c}{[x+\xi-i\varepsilon][x-\xi+i\varepsilon]},$$

where $c = (4\pi\alpha_s e e_Q R(0))/(m_Q^{3/2}\sqrt{2\pi N_c})$. $R_{J/\psi}(0) = 1$ GeV$^{3/2}$ and $R_\Upsilon(0) = 3$ GeV$^{3/2}$ from potential models and NLO decay widths.
In our calculation we use the complete NLO result for coefficient functions [Ivanov, Schafer, Szymanowsky, Krasnikov, 2004] .

GPDs:

$$F_{q,ss'} = \frac{1}{2}\int \frac{\mathrm{d}y^-}{2\pi} e^{ixP^+y^-} \langle p',s'|\bar{\psi}^q\left(\tfrac{-y}{2}\right)\gamma^+\psi^q\left(\tfrac{y}{2}\right)|p,s\rangle|_{y^+=y_\perp=0},$$

$$F_{g,ss'} = \frac{1}{P^+}\int \frac{\mathrm{d}y^-}{2\pi} e^{ixP^+y^-} \langle p',s'|F^{+\mu}\left(\tfrac{-y}{2}\right)F_\mu{}^+\left(\tfrac{y}{2}\right)|p,s\rangle|_{y^+=y_\perp=0},$$

are parametrised as $(j=g,q)$:

$$F_{j,ss'} = \frac{1}{2P^+}\left[\bar{u}_{s'}(p')\left(H_j\gamma^+ + E_j\frac{i\sigma^{+\Delta}}{2m_p}\right)u_s(p)\right].$$

GPD input

For numerical calcuations we use GPDs obtained as the result of **full LO GPD evolution** w.r.t. μ_F with initial condition at $\mu_0 = 2$ GeV, given by the double-distribution ansatz (without D-term):

$$H_i(x,\xi) = \int_{-1}^{1} d\beta \int_{-1+|\beta|}^{1-|\beta|} d\alpha\, \delta(\beta + \xi\alpha - x)\, f_i(\beta,\alpha)\,,$$

with the following model for DDs:

$$f_i(\beta,\alpha) = h_i(\beta,\alpha) \times \begin{cases} |\beta| g(|\beta|) & \text{for } i = g, \\ \theta(\beta) q_{\text{val}}(|\beta|) & \text{for valence } q, \\ \text{sgn}(\beta) q_{\text{sea}}(|\beta|) & \text{for sea } q. \end{cases}$$

where the profile function $h_i(\beta,\alpha) = \frac{\Gamma(2n_i+2)}{2^{2n_i+1}\Gamma^2(n_i+1)} \frac{\left((1-|\beta|)^2-\alpha^2\right)^{n_i}}{(1-|\beta|)^{2n_i+1}}$, with $n_g = n_q^{\text{sea}} = 2$ and $n_q^{\text{val}} = 1$ as in GK model. A range of values for n_g was tried with very small (few %) numerical effects on the cross section.

High-energy instability of NLO CF

The μ_F-dependence of the **LO** vs. **NLO** CF calculation:

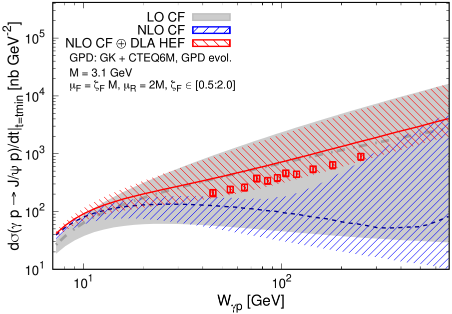

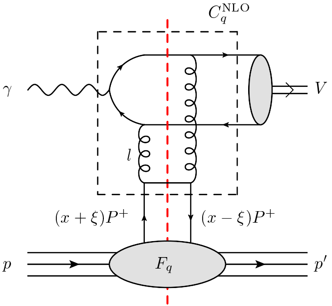

The instability is caused by the high-partonic-energy ($\xi \ll |x| \lesssim 1$) DGLAP region [Ivanov, 2007] :

$$\int_\xi^1 \frac{dx}{x^2} F_g(x,\xi,\mu_F) C^{(1)}(x,\xi) \sim \int_\xi^1 \frac{dx}{x} = \ln\frac{1}{\xi}, \text{ if } F_g(x) \sim \text{const. and } C^{(1)} \sim x.$$

And for $\xi \ll x$ we actually have:

$$C^{(1)}_{g,q}(x,\xi) \sim -\frac{i\pi|x|}{2\xi} \ln\left(\frac{M_{\mathcal{Q}}^2}{4\mu_F^2}\right) \times \left\{C_A, 2C_F\right\} \equiv C^{(1,\text{ asy.})}_{\{g,q\}}(x,\xi).$$

HEF for imaginary part of the amplitude

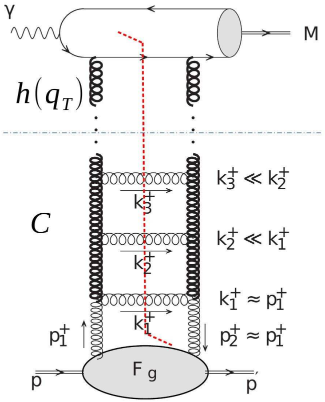

HEF-resummed result for the imaginary part in the DGLAP region [Ivanov, 2007] :

$$C_i^{(\mathrm{HEF})}(\rho) = \frac{-i\pi}{2}\frac{c}{|\rho|}\int_0^\infty d\mathbf{q}_T^2\, \mathcal{C}_{gi}(|\rho|, \mathbf{q}_T^2) h(\mathbf{q}_T^2),$$

where $\rho = \xi/x$ and (in the LO in v^2 and α_s):

$$h(\mathbf{q}_T^2) = \frac{M_\mathcal{Q}^2}{M_\mathcal{Q}^2 + 4\mathbf{q}_T^2}.$$

HEF-resummed coefficient function

Resummed coefficient function in N-space ($\gamma_N = \hat{\alpha}_s(\mu_R)/N$):

$$C_g^{(\mathrm{HEF})}(N) = \frac{-i\pi c}{2} \left(\frac{M_{\mathcal{Q}}^2}{4\mu_F^2}\right)^{\gamma_N} \frac{\pi\gamma_N}{\sin(\pi\gamma_N)}.$$

Resummed coefficient function in ρ-space:

$$\check{C}_g^{(\mathrm{HEF})}(\rho) = \frac{-i\pi c}{2} \frac{\hat{\alpha}_s}{|\rho|} \sqrt{\frac{L_\mu}{L_\rho}} \left\{ I_1\left(2\sqrt{L_\rho L_\mu}\right) - 2\sum_{k=1}^{\infty} \mathrm{Li}_{2k}(-1) \left(\frac{L_\rho}{L_\mu}\right)^k I_{2k-1}\left(2\sqrt{L_\rho L_\mu}\right) \right\},$$

where $L_\rho = \hat{\alpha}_s \ln 1/|\rho|$ and $L_\mu = \ln[M_{\mathcal{Q}}^2/(4\mu_F^2)]$.
The $\rho \ll 1$-behaviour is governed by the singularity at $N = \hat{\alpha}_s$:

$$\check{C}_g^{(\mathrm{HEF})}(\rho) \sim \rho^{-\hat{\alpha}_s},$$

so the *hard Pomeron intercept* in DLA is $\hat{\alpha}_s$, not $4\hat{\alpha}_s \ln 2$ like in the full LLA.

Matching of the CF NLO and HEF-resummed coefficient functions

The $C_g^{(\mathrm{HEF})}(\rho)$ can be expanded in α_s (up to overall factor $-i\pi c/2$):

$$\underbrace{\delta(|\rho|-1)}_{\mathrm{LO}} + \underbrace{\frac{\hat{\alpha}_s}{|\rho|}\ln\left(\frac{M_{\mathcal{Q}}^2}{4\mu_F^2}\right)}_{=\frac{\alpha_s}{\pi}C_g^{(1,\ \mathrm{asy.})}(x,\xi)} + \frac{\hat{\alpha}_s^2}{|\rho|}\ln\frac{1}{|\rho|}\left[\frac{\pi^2}{6}+\frac{1}{2}\ln^2\left(\frac{M_{\mathcal{Q}}^2}{4\mu_F^2}\right)\right] + O(\alpha_s^3),$$

To avoid double-counting with NLO, we use the following *subtractive matching prescription*:

$$C_{g,q}^{(\mathrm{match.})}(x,\xi) = C_{g,q}^{(0)}(x,\xi) + \frac{\alpha_s(\mu_R)}{\pi}C_{g,q}^{(1)}(x,\xi)$$
$$+\left[\check{C}_{g,q}^{(\mathrm{HEF})}(\xi/|x|) - \frac{\alpha_s(\mu_R)}{\pi}C_{g,q}^{(1,\ \mathrm{asy.})}(x,\xi)\right]\theta(|x|-\xi).$$

Numerical results, $\mu_R = 2M$, μ_F-variation

The μ_F-dependence of the **LO** vs. **NLO** CF and **NLO CF⊕DLA HEF matched** calculation:

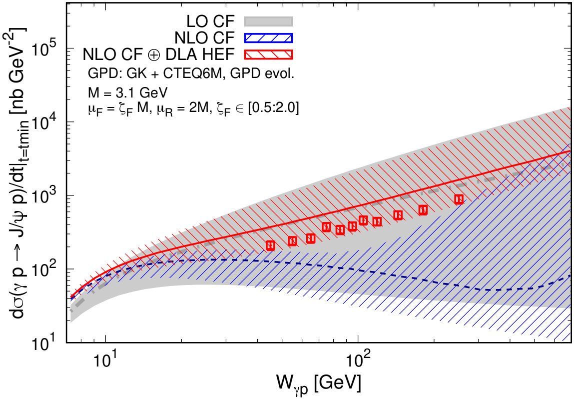

Points – H1 data on $d\sigma/dt$ at $t \simeq 0$.

Exclusive J/ψ photoproduction in CF⊕HEF

9-point μ_F and μ_R variation:

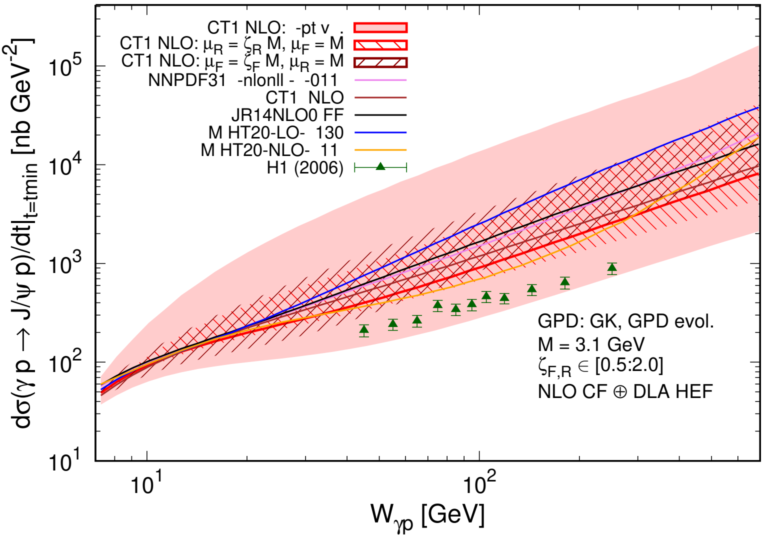

Exclusive J/ψ photoproduction in CF⊕HEF

Comparison to data on $d\sigma/dt(t_{\rm min})$, extrapolated from total cross section data at various energies:

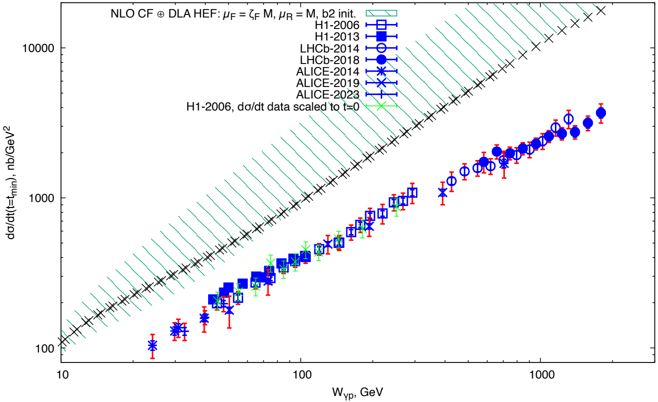

Results for $\Upsilon(1S)$

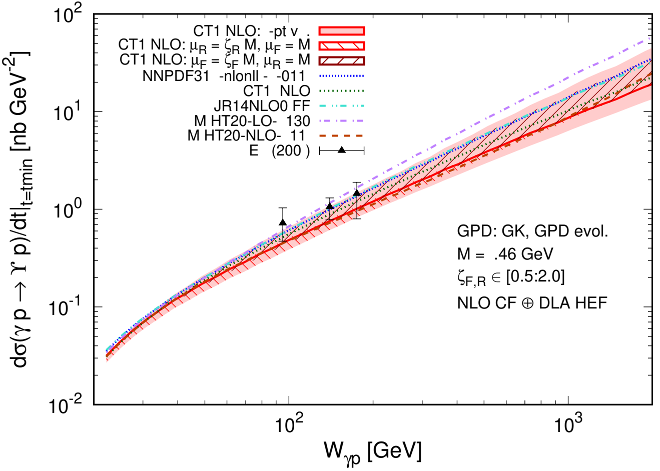

Plots from hep-ph/2204.14031 CGC calculation without and with $O(v^2)$-correction:

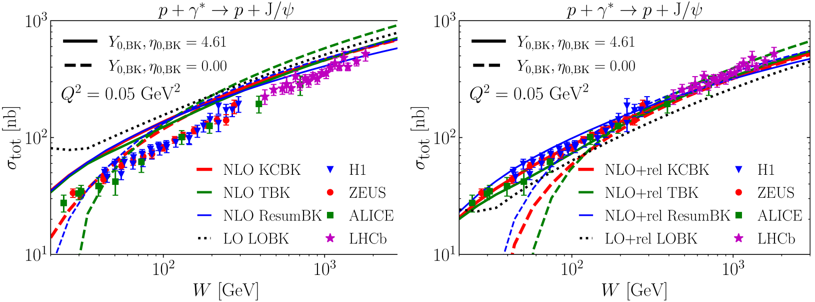

III. NLO impact-factor for the forward η_c hadroproduction

Inclusive heavy quarkonium production at moderate p_T in CF

It is well known that quarkonium production p_T spectra at $p_T \gtrsim M$ are not described by collinear factorisation computations at NLO. Example: η_c production at LHCb [LHCb, '24] (left panel $d\sigma/dp_T$, right panel: ratio to J/ψ):

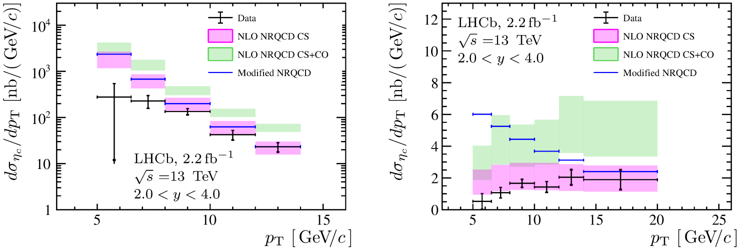

$p(P_1)+p(P_2) \to \eta_c(p)+X$, parton level e.g.: $g(x_1P_1) + g(x_2P_2) \to c\bar{c}[^1S_0^{[1]}] + X$,

with $S = (P_1 + P_2)^2$ and $p^2 = M^2$. Cross section in **collinear factorisaton**:

$$\frac{d\sigma}{d\mathbf{p}_T^2 dy} = \frac{M^2}{S} \int\limits_0^{\eta_{\max}} d\eta \int\limits_{z_{\min}}^{z_{\max}} dz \; f_i\left(\frac{M_T e^y}{\sqrt{S}z}, \mu_F\right) f_j\left(\frac{M^2 z(1+\eta)}{M_T\sqrt{S}} e^{-y}, \mu_F\right) \frac{d\hat{\sigma}_{ij}(\eta, z, \mathbf{p}_T^2)}{dz d\mathbf{p}_T^2},$$

where $\eta = \hat{s}/M^2 - 1$ with $\hat{s} = Sx_1x_2$, $z = \frac{p_+}{x_1 P_1^+}$, $M_T = \sqrt{M^2 + \mathbf{p}_T^2}$.

High-Energy Factorization, forward η_c hadroproduction

The **LLA** ($\sum_n \alpha_s^n \ln^{n-1}$) formalism [Collins, Ellis, '91; Catani, Ciafaloni, Hautmann, '91,'94]

Physical picture in the **LLA**:

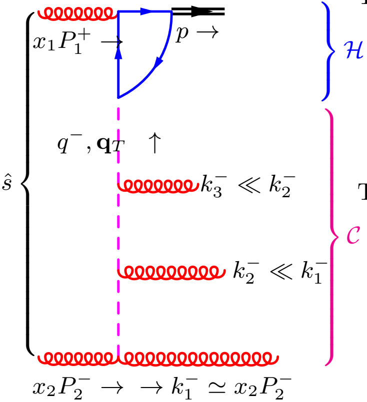

The LLA in $\ln(x_2 P_2^-/p^-)$:

$$\hat{\sigma}_{\rm HEF}(p_-/(x_2 P_2^-), z) \propto \int\limits_0^\infty dq^- \int\limits_0^\infty d\mathbf{q}_T^2 \mathcal{C}\left(\frac{q^-}{x_2 P_2^-}, \mathbf{q}_T^2, \mu_F, \mu_R\right) \mathcal{H}(q^-, \mathbf{q}_T^2, z),$$

The LLA in $\ln(\hat{s}/M^2)$:

$$\hat{\sigma}_{\rm HEF}(\hat{s}/M^2, z) \propto \int\limits_0^\infty d\mathbf{q}_T^2 \mathcal{C}\left(\frac{\hat{s}}{M^2}, \mathbf{q}_T^2, \mu_F, \mu_R\right) \int\limits_0^\infty dq^- \mathcal{H}(q^-, \mathbf{q}_T^2, z).$$

Two kinds of LLA are equivalent up to NLL terms because

$$\frac{\hat{s}}{M^2} = \frac{x_1 x_2 S}{M^2} = \frac{M^2 + \mathbf{p}_T^2}{M^2} \frac{x_2 P_2^-}{q^-} = \frac{M^2 + \mathbf{p}_T^2}{M^2} \frac{x_2 P_2^-}{p^-}.$$

The Leading Order

The LLA resummation formula for $\mathbf{p}_T^2$ and $z = p_-/q_-$-differential partonic cross section:

$$\frac{d\hat{\sigma}_{ig}^{(\mathrm{LLA})}}{dz d\mathbf{p}_T^2} = \frac{1}{2M^2}\int \frac{d^2\mathbf{q}_T}{\pi}\mathcal{C}_{ig}\left(\frac{\hat{s}}{M^2}, \mathbf{q}_T^2, \mu_F, \mu_R\right)\mathcal{H}_{gg}^{(\mathrm{LO})}(\mathbf{q}_T^2, z, \mathbf{p}_T^2),$$

$$= \frac{1}{2M^2}\mathcal{C}_{ig}\left(\frac{\hat{s}}{M^2}, \mathbf{p}_T^2, \mu_F, \mu_R\right)\mathcal{H}_{gg}^{(\mathrm{LO})}(\mathbf{p}_T^2)\delta(1-z),$$

with [Kniehl, Vasin, Saleev, '06]

$$\mathcal{H}_{gg}^{(\mathrm{LO})} = \frac{32\pi^3\alpha_s^2(\mu_R)M^4}{N_c^2(N_c^2-1)(M^2+\mathbf{p}_T^2)^2}\frac{\left\langle \mathcal{O}\left[{}^1S_0^{[1]}\right]\right\rangle}{M^3}\delta(1-z)\delta(\mathbf{q}_T^2-\mathbf{p}_T^2),$$

where $\left\langle \mathcal{O}\left[{}^1S_0^{[1]}\right]\right\rangle = 2N_c|R(0)|^2/(4\pi)$.

In this talk we will compute $\mathcal{H}_{gg}^{(\mathrm{NLO})}(\mathbf{q}_T^2, z, \mathbf{p}_T^2)$, which includes **virtual** and **real-emission** corrections.

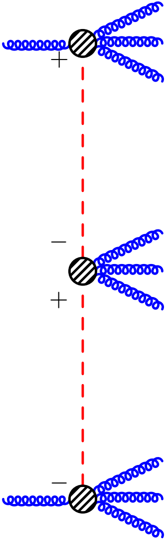

- Reggeized gluon fields $R_\pm$ carry $(k_\pm, \mathbf{k}_T, k_\mp = 0)$: $\partial_\mp R_\pm = 0$.
- **Induced interactions** of particles and Reggeons [Lipatov '95, '97; Bondarenko, Zubkov '18]:

$$L = \frac{i}{g_s} \mathrm{tr}\left[R_+ \partial_\perp^2 \partial_- \left(W\left[A_-\right] - W^\dagger\left[A_-\right]\right) + (+ \leftrightarrow -)\right],$$

with $W_{x_\mp}[x_\pm, \mathbf{x}_T, A_\pm] = P \exp\left[\frac{-ig_s}{2} \int\limits_{-\infty}^{x_\mp} dx'_\mp A_\pm(x_\pm, x'_\mp, \mathbf{x}_T)\right] = \left(1 + ig_s \partial_\pm^{-1} A_\pm\right)^{-1}$.

- Expansion of the Wilson line generates **induced vertices**:

$$\mathrm{tr}\left[R_+ \partial_\perp^2 A_- + (-ig_s)(\partial_\perp^2 R_+)(A_- \partial_-^{-1} A_-) \right.$$
$$\left. + (-ig_s)^2 (\partial_\perp^2 R_+)(A_- \partial_-^{-1} A_- \partial_-^{-1} A_-) + O(g_s^3) + (+ \leftrightarrow -)\right].$$

- The *Eikonal propagators* $\partial_\pm^{-1} \to -i/(k^\pm)$ lead to **rapidity divergences**, which are regularized by tilting the Wilson lines from the light-cone [Hentschinski, Sabio Vera, Chachamis *et. al.*, '12-'13; M.N. '19]:

$$n_\pm^\mu \to \tilde{n}_\pm^\mu = n_\pm^\mu + r n_\mp^\mu, \; r \ll 1 : \; \tilde{k}^\pm = \tilde{n}^\pm k.$$

The terms for conversion of the result into any other regularisation scheme for RDs can be easily computed.

$Rg \to c\bar{c}\left[{}^1S_0^{[1]}\right]$ and $c\bar{c}\left[{}^3S_1^{[8]}\right]$ @ 1 loop

Interference with LO: 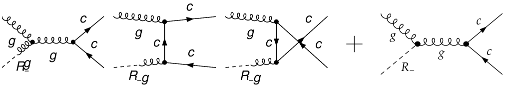

Induced Rgg coupling diagrams:

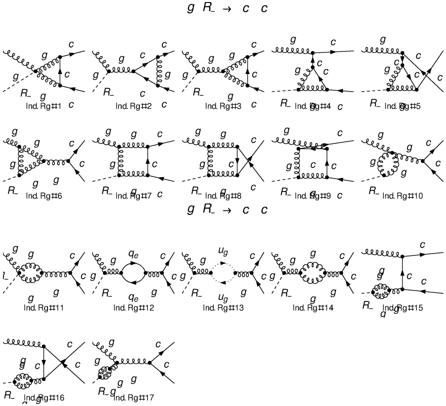

Some Rg-coupling diagrams:

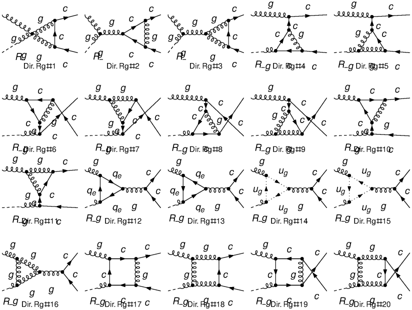

and so on...

- Diagrams had been generated using custom **FeynArts** model-file, projector on the $c\bar{c}\left[{}^1S_0^{[1]}\right]$-state is inserted
- heavy-quark momenta $= p_{\mathcal{Q}}/2 \Rightarrow$ need to resolve linear dependence of quadratic denominators in some diagrams before IBP
- IBP reduction to master integrals has been performed using **FIRE**
- Master integrals with linear and massless quadratic denominators are expanded in $r \ll 1$ using Mellin-Barnes representation. The differential equations technique is used when the integral depends on more than one scale of virtuality.
- In presence of the linear denominator the massive propagator can be converted to the massless one:

$$\frac{1}{((\tilde{n}_+ l) + k_+)(l^2 - m^2)} = \frac{1}{((\tilde{n}_+ l) + k_+)(l + \kappa \tilde{n}_+)^2} + \frac{2\kappa\left[(\tilde{n}_+ l) + \frac{m^2 + \tilde{n}_+^2 \kappa^2}{2\kappa}\right]}{((\tilde{n}_+ l) + k_+)(l + \kappa \tilde{n}_+)^2 (l^2 - m^2)}$$

$\Rightarrow$ all the masses can be moved to integrals with **only quadratic propagators**.

See [hep-ph/2408.06234] for details.

Result: $Rg \to c\bar{c}\left[{}^1S_0^{[1]}\right]$ @ 1 loop

Result [MN, '23, '24] for $2\Re\left[\frac{H_{1L\times LO}(\mathbf{q}_T)-(\text{On-shell mass CT})}{(\alpha_s/(2\pi))H_{LO}(\mathbf{q}_T)}\right]$:

$$\left(\frac{\mu^2}{\mathbf{q}_T^2}\right)^{\epsilon}\left\{-\frac{N_c}{\epsilon^2}+\frac{1}{\epsilon}\left[N_c\left(\ln\frac{(x_1P_1^+)^2}{\mathbf{q}_T^2 r}+\frac{25}{6}\right)-\frac{2n_F}{3}-\frac{3}{2N_c}\right]\right\}-\frac{10}{9}n_F+F_{{}^1S_0^{[1]}}(\mathbf{q}_T^2/M^2)$$

Cross-check against the Regge limit of one-loop amplitude ($\tau=\mathbf{q}_T^2/M^2$):

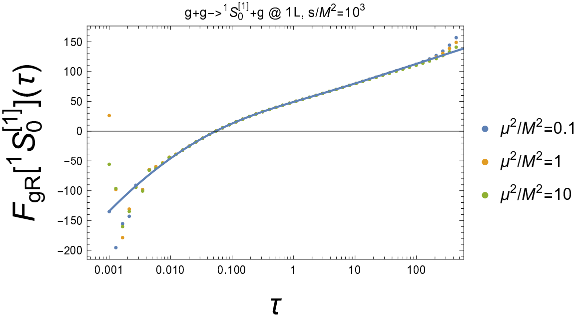

Points – the function $F_{{}^1S_0^{[1]}}(\tau)$ extracted form numerical results for interference between **exact** one-loop and tree-level QCD amplitudes of $g+g\to c\bar{c}[{}^1S_0^{[1]}]+g$ at $s=10^3M^2$. Solid line – analytic result from the EFT.

Real-emission correction

The real-emission contribution:

$$g(x_1 P_1) + R_-(q) \to c\bar{c}[^1S_0^{[1]}](p) + g(k),$$

to the coefficient function is given by:

$$\mathcal{H}_{gg}^{(\text{NLO, R})}(\mathbf{q}_T^2, z, \mathbf{p}_T^2) = \frac{\alpha_s(\mu_R)}{2\pi}\mathcal{H}_{gg}^{(\text{LO})}(\mathbf{p}_T^2)\int \frac{d\Omega_{2-2\epsilon}}{(2\pi)^{1-2\epsilon}}\frac{\tilde{H}_{Rg}(\mathbf{q}_T, \mathbf{p}_T, z)}{z(1-z)\mathbf{q}_T^2},$$

where the **function** $\tilde{H}_{Rg}(\mathbf{q}_T, \mathbf{p}_T, z)$ **is very complicated.** The following subtraction term ($O(\epsilon)$ terms not shown):

$$\mathcal{J}_{Rj}^{(\text{sub.})} = \frac{2C_A}{\mathbf{k}_T^2}\left[\frac{1-z}{(1-z)^2 + r\frac{\mathbf{k}_T^2}{(x_1 P_1^+)^2}} + \Delta p_{gg}(z, \mathbf{q}_T, \mathbf{p}_T)\right],$$

where $\Delta p_{gg} = z(1-z) + 2\frac{\mathbf{k}_T^2\mathbf{p}_T^2 - (\mathbf{k}_T\mathbf{p}_T)^2}{z\mathbf{k}_T^2\mathbf{p}_T^2} - \frac{3\mathbf{k}_T^2\mathbf{p}_T^2 - 2(\mathbf{k}_T\mathbf{p}_T)^2}{\mathbf{k}_T^2\mathbf{p}_T^2}$. captures it's singular behaviour in:

- **Regge limit:** $z \to 1$, $\mathbf{k}_T = \mathbf{q}_T - \mathbf{p}_T$ – fixed,
- **Collinear limit:** $\mathbf{k}_T \to 0$, z-fixed
- **Soft limit:** $\mathbf{k}_T \to 0$, $z \to 1$

Real-emission correction, finite part

$$\mathcal{H}^{(\mathrm{fin.})}_{gj}(\mathbf{q}_T^2, z, \mathbf{p}_T^2) = \frac{\alpha_s(\mu_R)}{2\pi}\mathcal{H}^{(\mathrm{LO})}_{gg}(\mathbf{p}_T^2)\int\limits_0^{2\pi}\frac{d\phi}{2\pi}\left[\frac{\tilde{H}_{Rj}(\mathbf{q}_T, \mathbf{p}_T, z)}{z(1-z)\mathbf{q}_T^2} - \mathcal{J}^{(\mathrm{sub.})}_{Rj}(\mathbf{q}_T, \mathbf{p}_T, z, r=0)\right]$$

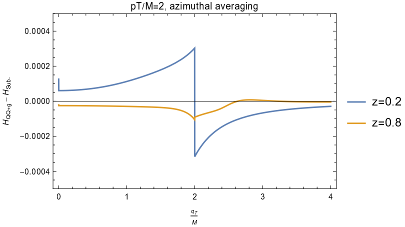

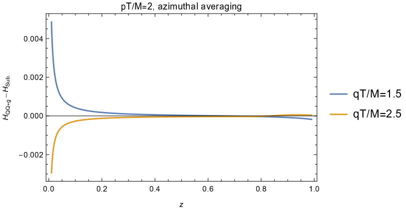

This contribution is finite for $\mathbf{k}_T \to 0$ and $z \to 1$ and can be safely convoluted with the resummation factor or unintegrqted-PDF in $\mathbf{q}_T$ and gluon PDF in z.

Integrated subtraction term

$$\mathcal{H}_{gj}^{(\text{int. sub.})}(\mathbf{q}_T^2, z, \mathbf{p}_T^2) = \frac{\alpha_s(\mu_R)}{2\pi}\frac{\Omega_{2-2\epsilon}\mu^{2\epsilon}}{(2\pi)^{1-2\epsilon}}\int d^{2-2\epsilon}\mathbf{k}_T \mathcal{J}_{Rj}^{(\text{sub.})}(\mathbf{q}_T, \mathbf{q}_T - \mathbf{k}_T, z, r)$$

$$\times \mathcal{H}_{gg}^{(\text{LO})}(\mathbf{q}_T - \mathbf{k}_T, \mathbf{p}_T) = \mathcal{H}_{gj}^{(\text{int. sub. I})} + \mathcal{H}_{gj}^{(\text{int. sub. II})}$$

$$\mathcal{H}_{gj}^{(\text{int. sub. I})} = \frac{\alpha_s(\mu_R)C_A}{\pi}\int \frac{d^2\mathbf{k}_T}{\mathbf{k}_T^2}\left[\frac{1}{(1-z)_+} + \Delta p_{gg}(z, \mathbf{q}_T, \mathbf{p}_T)\right.$$

$$\left. -\delta(1-z)\frac{1}{2}\ln\frac{r\mathbf{k}_T^2}{(x_1 P_1^+)^2}\right]\left[\delta^{(2)}(\mathbf{q}_T - \mathbf{k}_T - \mathbf{p}_T) - \frac{\mathbf{p}_T^2}{\mathbf{p}_T^2 + \mathbf{k}_T^2}\delta^{(2)}(\mathbf{q}_T - \mathbf{p}_T)\right]\mathcal{H}_{gg}^{(\text{LO})}(\mathbf{p}_T^2)$$

$$\mathcal{H}_{gj}^{(\text{int. sub. II})} = \frac{\alpha_s(\mu_R)}{2\pi}\mathcal{H}_{gg}^{(\text{LO})}(\mathbf{p}_T^2)\delta(\mathbf{p}_T^2 - \mathbf{q}_T^2)\frac{(4\pi)^\epsilon}{\Gamma(1-\epsilon)}\left(\frac{\mu^2}{\mathbf{p}_T^2}\right)^\epsilon$$

$$\times\left\{-\frac{1}{\epsilon}P_{gg}(z) + \delta(1-z)\left[\frac{C_A}{\epsilon^2} + \frac{\beta_0}{2}\frac{1}{\epsilon} + \frac{C_A}{\epsilon}\ln\frac{r\mathbf{p}_T^2}{(x_1 P_1^+)^2} - \frac{\pi^2}{6}C_A\right] + O(\epsilon^2)\right\}.$$

Rapidity factorisation schemes

The $\ln r$-regularisation is equivalent to the cut in rapidity, **for HEF** we need to cut in "target light-cone component" k_-:

$$\mathcal{H}_{gj}^{(\text{HEF-sch.})}(\mathbf{q}_T^2, z, \mathbf{p}_T^2) = \frac{\bar{\alpha}_s}{2\pi}\mathcal{H}_{gg}^{(\text{LO})}(\mathbf{q}_T^2, \mathbf{p}_T^2, z)\left[-\frac{1}{\epsilon}\left(\frac{\beta_0}{2} - C_A\right) + \frac{4}{3}C_A - \frac{5}{6}\beta_0 - \frac{\pi^2}{3}C_A\right]$$
$$-\frac{\alpha_s C_A}{\pi}\mathcal{H}_{gg}^{(\text{LO})}(\mathbf{p}_T^2)\int\frac{d^2\mathbf{k}_T}{\mathbf{k}_T^2}\left[\delta^{(2)}(\mathbf{q}_T - \mathbf{k}_T - \mathbf{p}_T) - \frac{\mathbf{p}_T^2}{\mathbf{p}_T^2 + \mathbf{k}_T^2}\delta^{(2)}(\mathbf{q}_T - \mathbf{p}_T)\right]$$
$$\times\left(-\frac{1}{2}\ln r + \ln\frac{|\mathbf{k}_T|}{\Lambda_-}\right),$$

where $\Lambda_- \simeq q_- = (M^2 + \mathbf{p}_T^2)/(x_1 P_1^+)$. The **blue** terms come from R self-energy.

In BFKL we cut in $\ln(s_{\eta_c g}/s_0)$:

$$\mathcal{H}_{gj}^{(\text{BFKL-sch.})}(\mathbf{q}_T^2, z, \mathbf{p}_T^2) = \frac{\bar{\alpha}_s}{2\pi}\mathcal{H}_{gg}^{(\text{LO})}(\mathbf{q}_T^2, \mathbf{p}_T^2, z)\left[-\frac{1}{\epsilon}\left(\frac{\beta_0}{2} - C_A\right) + \frac{4}{3}C_A - \frac{5}{6}\beta_0\right]$$
$$-\frac{\alpha_s C_A}{\pi}\mathcal{H}_{gg}^{(\text{LO})}(\mathbf{p}_T^2)\int\frac{d^2\mathbf{k}_T}{\mathbf{k}_T^2}\left[\delta^{(2)}(\mathbf{q}_T - \mathbf{k}_T - \mathbf{p}_T) - \frac{\mathbf{p}_T^2}{\mathbf{p}_T^2 + \mathbf{k}_T^2}\delta^{(2)}(\mathbf{q}_T - \mathbf{p}_T)\right]$$
$$\times\left(-\frac{1}{2}\ln r + \ln\frac{x_1 P_1^+}{\sqrt{s_0}}\right).$$

Impact factor, HEF scheme

$$\mathcal{H}_{gg}^{(\text{NLO, analyt.})}(\mathbf{q}_T, z, \mathbf{p}_T) = \mathcal{H}_{gj}^{(\text{int. sub. I})} + \mathcal{H}_{gj}^{(\text{int. sub. II})} + \mathcal{H}_{gj}^{(\text{NLO, V})} + \mathcal{H}_{gj}^{(\text{HEF-sch.})}$$

$$= \frac{\alpha_s C_A}{\pi} \mathcal{H}_{gg}^{(\text{LO})}(\mathbf{p}_T^2) \int \frac{d^2\mathbf{k}_T}{\mathbf{k}_T^2} \left[\delta^{(2)}(\mathbf{q}_T - \mathbf{k}_T - \mathbf{p}_T) - \frac{\mathbf{p}_T^2}{\mathbf{p}_T^2 + \mathbf{k}_T^2} \delta^{(2)}(\mathbf{q}_T - \mathbf{p}_T) \right] \left[\frac{1}{(1-z)_+} \right.$$

$$\left. + z(1-z) + 2\frac{\mathbf{k}_T^2 \mathbf{p}_T^2 - (\mathbf{k}_T \mathbf{p}_T)^2}{z \mathbf{k}_T^2 \mathbf{p}_T^2} - \frac{3\mathbf{k}_T^2 \mathbf{p}_T^2 - 2(\mathbf{k}_T \mathbf{p}_T)^2}{\mathbf{k}_T^2 \mathbf{p}_T^2} + \delta(1-z) \ln\left(\frac{M^2 + \mathbf{p}_T^2}{\mathbf{k}_T^2}\right) \right]$$

$$+ \frac{\alpha_s C_A}{2\pi} \mathcal{H}_{gg}^{(\text{LO})}(\mathbf{p}_T^2) \delta(\mathbf{q}_T^2 - \mathbf{p}_T^2) \left\{ -\ln \frac{\mu_F^2}{\mathbf{p}_T^2} P_{gg}(z) \right.$$

$$\left. + \delta(1-z) \left[-\frac{\pi^2}{2} C_A + \frac{4}{3} C_A - \frac{5}{6}\beta_0 - 2C_F \left(2 + \frac{2}{3} \ln \frac{\mathbf{p}_T^2}{m_c^2} \right) + \beta_0 \ln \frac{\mu_R^2}{\mathbf{p}_T^2} + F_{{}^1S_0^{[1]}}(\mathbf{p}_T^2/M^2) \right] \right\}$$

This result should be added to the $\mathcal{H}_{gg}^{(\text{fin.})}$.

Impact factor, BFKL scheme

$$
\begin{aligned}
&\mathcal{H}_{gg}^{(\text{NLO, analyt., BFKL})}(\mathbf{q}_T, z, \mathbf{p}_T) = \mathcal{H}_{gj}^{(\text{int. sub. I})} + \mathcal{H}_{gj}^{(\text{int. sub. II})} + \mathcal{H}_{gj}^{(\text{NLO, V})} + \mathcal{H}_{gj}^{(\text{BFKL-sch.})} \\
&= \frac{\alpha_s C_A}{\pi} \mathcal{H}_{gg}^{(\text{LO})}(\mathbf{p}_T^2) \int \frac{d^2\mathbf{k}_T}{\mathbf{k}_T^2} \left[\delta^{(2)}(\mathbf{q}_T - \mathbf{k}_T - \mathbf{p}_T) - \frac{\mathbf{p}_T^2}{\mathbf{p}_T^2 + \mathbf{k}_T^2} \delta^{(2)}(\mathbf{q}_T - \mathbf{p}_T) \right] \left[\frac{1}{(1-z)_+} \right. \\
&\left. + z(1-z) + 2\frac{\mathbf{k}_T^2 \mathbf{p}_T^2 - (\mathbf{k}_T \mathbf{p}_T)^2}{z \mathbf{k}_T^2 \mathbf{p}_T^2} - \frac{3\mathbf{k}_T^2 \mathbf{p}_T^2 - 2(\mathbf{k}_T \mathbf{p}_T)^2}{\mathbf{k}_T^2 \mathbf{p}_T^2} + \delta(1-z) \ln\left(\frac{\sqrt{s_0}}{|\mathbf{k}_T|} \right) \right] \\
&\qquad + \frac{\alpha_s C_A}{2\pi} \mathcal{H}_{gg}^{(\text{LO})}(\mathbf{p}_T^2) \delta(\mathbf{q}_T^2 - \mathbf{p}_T^2) \left\{ -\ln \frac{\mu_F^2}{\mathbf{p}_T^2} P_{gg}(z) \right. \\
&\left. + \delta(1-z) \left[-\frac{\pi^2}{6} C_A + \frac{4}{3} C_A - \frac{5}{6}\beta_0 - 2C_F \left(2 + \frac{2}{3} \ln \frac{\mathbf{p}_T^2}{m_c^2} \right) + \beta_0 \ln \frac{\mu_R^2}{\mathbf{p}_T^2} + F_{{}^1S_0^{[1]}}(\mathbf{p}_T^2/M^2) \right] \right\}
\end{aligned}
$$

This result should be added to **the same** $\mathcal{H}_{gg}^{(\text{fin.})}$.

Impact factor, $q+R$ channel

$$
\begin{aligned}
&\mathcal{H}_{qg}^{(\text{NLO, analyt.})}(\mathbf{q}_T, z, \mathbf{p}_T) \\
&= \frac{\alpha_s C_F}{2\pi}\mathcal{H}_{gg}^{(\text{LO})}(\mathbf{p}_T^2)\int \frac{d^2\mathbf{k}_T}{\mathbf{k}_T^2}\left[\delta^{(2)}(\mathbf{q}_T-\mathbf{k}_T-\mathbf{p}_T)-\frac{\mathbf{p}_T^2}{\mathbf{p}_T^2+\mathbf{k}_T^2}\delta^{(2)}(\mathbf{q}_T-\mathbf{p}_T)\right] \\
&\times\left[\frac{(2-z)^2}{z}-\frac{4(1-z)}{z}\frac{(\mathbf{k}_T\mathbf{p}_T)^2}{\mathbf{k}_T^2\mathbf{p}_T^2}\right] \\
&\qquad +\frac{\alpha_s}{2\pi}\mathcal{H}_{gg}^{(\text{LO})}(\mathbf{p}_T^2)\delta(\mathbf{q}_T^2-\mathbf{p}_T^2)\left\{-\ln\frac{\mu_F^2}{\mathbf{p}_T^2}P_{gq}(z)+C_F z\right\}.
\end{aligned}
$$

This result should be added to $\mathcal{H}_{qg}^{(\text{fin.})}$ computed using the subtraction term ($O(\epsilon)$ terms are not shown):

$$
\mathcal{J}_{qg} = \frac{C_F}{z\mathbf{k}_T^2}\left[(2-z)^2-4(1-z)\frac{(\mathbf{k}_T\mathbf{p}_T)^2}{\mathbf{k}_T^2\mathbf{p}_T^2}\right],
$$

together with the complete NLO matrix element of the process $q+R\to q+g$: $\tilde{H}_{Rq}$.

Numerical cross-check against NLO CF computation ($q+g$ channel)

Expansion of the NLL HEF result should reproduce the $\hat{s} \gg M^2$ asymptotics of the full NLO CF computation:

$$\left.\frac{d\hat{\sigma}^{(\mathrm{LO+NLO})}_{qg}}{dz\, d\mathbf{p}_T^2}\right|_{\hat{s}\gg M^2} = \frac{\hat{\alpha}_s}{\mathbf{q}_T^2} \widetilde{\otimes} \mathcal{H}^{(\mathrm{NLO})}_{qg}$$

$$= \hat{\alpha}_s \int \frac{d^2\mathbf{q}_T}{\pi \mathbf{q}_T^2} \left[\mathcal{H}^{(\mathrm{NLO})}_{qg}(\mathbf{q}_T, z, \mathbf{p}_T) - \mathcal{H}^{(\mathrm{NLO})}_{qg}(0, z, \mathbf{p}_T)\theta(\mu_F^2 - \mathbf{q}_T^2)\right].$$

Preliminary numerical comparison ($\mu_R = \mu_F = \sqrt{M^2 + p_T^2}$):

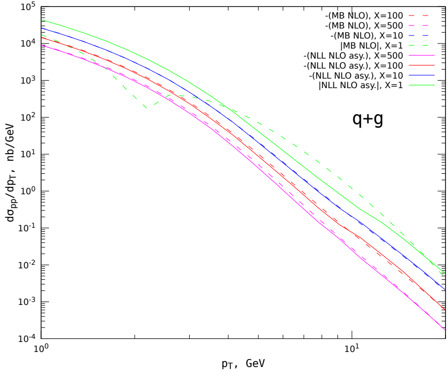

Dashed lines – NLO CF results by *M. Butenschön*, solid lines – NLL HEF prediction.

The NLO CF computation is done with the cut on $\hat{s} > X\hat{s}_{\min}$ with $\hat{s}_{\min} = 2M_T[M_T + |\mathbf{p}_T|] - M^2$ – kilematical lower bound of $\hat{s}$ for given p_T.

Green – $X = 1$, blue – $X = 10$ and red – $X = 100$, magenta – $X = 500$.

Resummation function beyond DLA

The NLO result for the resummation function $\mathcal{C}_{gg}(x, \mathbf{q}_T, \mu_F, \mu_R)$ (1-loop virtual $g + R \to g$ + real $g + R \to g + g$ and $g + R \to q + \bar{q}$):

$$\mathcal{C}_{gg}^{(\mathrm{NLO})} = \frac{\hat{\alpha}_s^2}{\mathbf{q}_T^2} \left[\ln \frac{1}{x} \ln \frac{\mathbf{q}_T^2}{\mu_F^2} + \left(\frac{11}{12} - \frac{n_F}{6N_c} \right) \ln \frac{\mu_R^2}{\mu_F^2} + \left(\frac{n_F}{6N_c} - \frac{n_F}{6N_c^3} - \frac{11}{6} \right) \ln \frac{\mathbf{q}_T^2}{\mu_F^2} + R_{gg}^{(2)} \right],$$

where $R_{gg}^{(2)} = \frac{67}{36} - \frac{5n_F}{18N_c} - \frac{n_F}{12N_c^3}$, $\hat{\alpha}_s = \alpha_s(\mu_R) C_A / \pi$.

The **DLA** resums corrections $\sim \hat{\alpha}_s \left(\hat{\alpha}_s \ln \frac{1}{x} \ln \frac{\mathbf{q}_T^2}{\mu_F} \right)^n$. The **NDLA** has one $\ln 1/x$ or $\ln \mu_F^2$ less per power of α_s. The resummed expression in NDLA can be obtained from RG analysis (running of α_s+collinear factorisation/DGLAP, $n_F = 0$):

$$\mathcal{C}_{gg}^{(\mathrm{NDLA})} = \left(1 + 4C_A a_s R_{gg}^{(2)} \right) \left[1 + a_s \beta_0 \ln \frac{\mu_R^2}{\mu_F^2} \left(1 + \ln \frac{\mu_F^2}{\mathbf{q}_T^2} \frac{\partial}{\partial \ln \mu_F^2} \right) + a_s \ln \frac{\mu_F^2}{\mathbf{q}_T^2} \left(\frac{22 C_A}{3} + \frac{\beta_0}{2} \ln \frac{\mu_F^2}{\mathbf{q}_T^2} \frac{\partial}{\partial \ln \mu_F^2} \right) \right] \mathcal{C}_{gg}^{(\mathrm{DLA})}(x, \mathbf{q}_T^2, \mu_F, \mu_R),$$

where $a_s = \alpha_s(\mu_R)/(4\pi)$.

Numerical cross-check against NLO CF computation ($g+g$ channel)

Expansion of the NLL HEF result should reproduce the $\hat{s} \gg M^2$ asymptotics of the full NLO CF computation:

$$\left.\frac{d\hat{\sigma}_{gg}^{(\mathrm{LO+NLO})}}{dz\,d\mathbf{p}_T^2}\right|_{\hat{s}\gg M^2} = \frac{\hat{\alpha}_s}{\mathbf{p}_T^2}\left[1+\hat{\alpha}_s \ln\frac{\hat{s}}{M_T^2}\ln\frac{\mu_F^2}{\mathbf{p}_T^2} + (\mathrm{NDLA}\ \mathcal{C})\right]\mathcal{H}_{gg}^{(\mathrm{LO})} + \frac{\hat{\alpha}_s}{\mathbf{q}_T^2}\widetilde{\otimes}\mathcal{H}_{gg}^{(\mathrm{NLO})}.$$

Preliminary numerical comparison ($\mu_R = \mu_F = \sqrt{M^2+p_T^2}$):

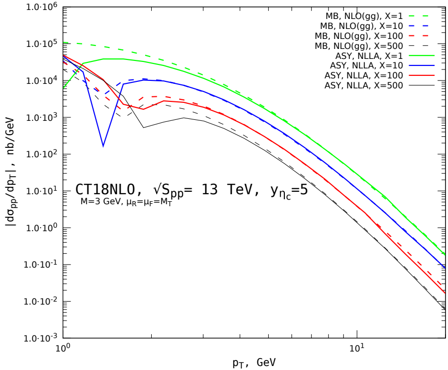

Dashed lines – NLO CF results by *M. Butenschön*, solid lines – NLL HEF prediction.
The NLO CF computation is done with the cut on $\hat{s} > X\hat{s}_{\min}$ with $\hat{s}_{\min} = 2M_T[M_T + |\mathbf{p}_T|] - M^2$ – kilematical lower bound of $\hat{s}$ for given p_T.
Green – $X=1$, blue – $X=10$ and red – $X=100$, black – $X=500$.

Numerical cross-check against NLO CF computation ($g + g$ channel)

Expansion of the NLL HEF result should reproduce the $\hat{s} \gg M^2$ asymptotics of the full NLO CF computation:

$$\left. \frac{d\hat{\sigma}_{gg}^{(\mathrm{LO+NLO})}}{dz d\mathbf{p}_T^2} \right|_{\hat{s} \gg M^2} = \frac{\hat{\alpha}_s}{\mathbf{p}_T^2} \left[1 + \hat{\alpha}_s \ln \frac{\hat{s}}{M_T^2} \ln \frac{\mu_F^2}{\mathbf{p}_T^2} + (\mathrm{NDLA}\ \mathcal{C}) \right] \mathcal{H}_{gg}^{(\mathrm{LO})} + \frac{\hat{\alpha}_s}{\mathbf{q}_T^2} \widetilde{\otimes} \mathcal{H}_{gg}^{(\mathrm{NLO})}.$$

Preliminary numerical comparison ($\mu_R = \mu_F = p_T$):

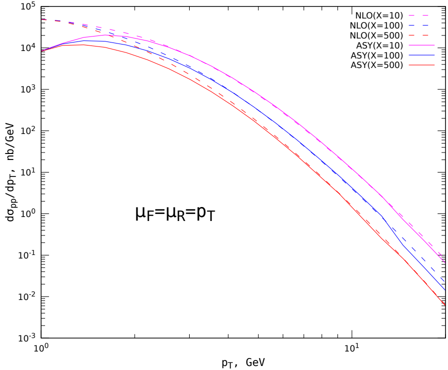

Dashed lines – NLO CF results by *M. Butenschön*, solid lines – NLL HEF prediction.
The NLO CF computation is done with the cut on $\hat{s} > X\hat{s}_{\min}$ with $\hat{s}_{\min} = 2M_T[M_T + |\mathbf{p}_T|] - M^2$ – kilematical lower bound of $\hat{s}$ for given p_T.
Magenta – $X = 10$ and blue – $X = 100$, red – $X = 500$.

Numerical cross-check against NLO CF computation ($g + g$ channel)

Constraining $\hat{s}$ from both sides:

$$X_1 < \frac{\hat{s}}{\hat{s}_{\min}} < X_2.$$

$\mu_R = \mu_F = \sqrt{M^2 + p_T^2}$

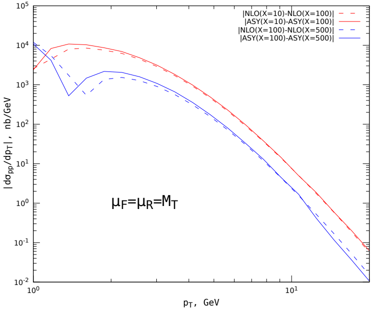

$\mu_R = \mu_F = p_T$

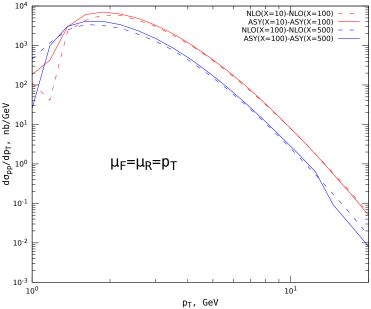

Red – $10 < \hat{s}/\hat{s}_{\min} < 100$, blue – $100 < \hat{s}/\hat{s}_{\min} < 500$. Solid lines – HEF prediction, dashed lines – NLO CF.

Conclusions and outlook

- The complete NLO HEF coefficient function (impact factor) for the $g + R \to c\bar{c}[^1S_0^{[1]}]$ process is computed, including one-loop and real-emission corrections
- The computation for other NRQCD-factorisation intermediate states: $c\bar{c}[^1S_0^{[8]}, {}^3S_1^{[8]}, {}^3P_J^{[1,8]}]$ are in progress. The $c\bar{c}[^3S_1^{[1]}]$ is more challenging.
- The result in HEF scheme is useful for the resummation of $\ln \hat{s}/M^2$ corrections in CF coefficient function
- The result in BFKL scheme is useful for the study of double-η_c froduction at large rapidity separation
- The result in the "shockwave" scheme, corresponding to the cut in "projectile" light-cone component (k^+) is easy to obtain. However this is $1R$-exchange only.
- The same computaion technology can be applied to the central production vertices $RR \to c\bar{c}[n]$.

Thank you for your attention!

The C_F coefficient

$$C_{gR}[{}^1S_0^{[8]}, C_F] = \frac{1}{6(\tau+1)^2}\Bigg\{-12\tau(\tau+1)\mathrm{Li}_2(-2\tau-1) + \frac{6L_2}{\tau}(-2L_1\tau + L_1 + 6\tau(\tau+1))$$

$$+\frac{1}{(2\tau+1)^2}\Bigg[(\tau+1)12\ln(2)(\tau+1)\left(6\tau^2+8\tau+3\right) - 8\tau^3\left(9\ln(\tau+1)+2\pi^2+15\right)$$

$$-4\tau^2\left(30\ln(\tau+1)+\pi^2+63\right) + 8\tau\left(-6\ln(\tau+1)+\pi^2-21\right)$$

$$+18(\tau+1)(2\tau+1)^2\ln(\tau) + 3\pi^2 - 36\Bigg]\Bigg\},$$

where $L_1 = L_1^{(+)} - L_1^{(-)} - L_2/2$ with $L_1^{(\pm)} = \sqrt{\tau(1+\tau)}\ln\left(\sqrt{1+\tau} \pm \sqrt{\tau}\right)$ and $L_2 = \sqrt{\tau(1+\tau)}\ln\left(1+2\tau+2\sqrt{\tau(1+\tau)}\right)$.

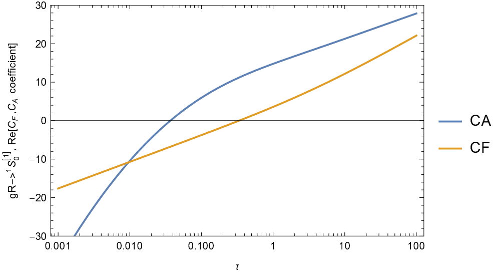

The C_A coefficient for $gR \to c\bar{c}\left[{}^1S_0^{[1]}\right]$

$$
\begin{aligned}
C_{gR}[{}^1S_0^{[1]}, C_A] &= \frac{2(\tau(\tau(\tau(7\tau+8)+2)-4)-1)}{(\tau-1)(\tau+1)^3}\mathrm{Li}_2(-\tau) \\
&-\frac{\tau(\tau(4\tau+5)+3)}{(\tau+1)^3}\mathrm{Li}_2(-2\tau-1) - \frac{L_2^2}{2\tau(\tau+1)^2} \\
&+\frac{1}{18(\tau-1)(\tau+1)^3}\Bigg\{-2\left(\tau^2-1\right)(18\ln(2)(\tau-1)\tau - 67(\tau+2)\tau - 67) \\
&+18[\ln(\tau)\left(-2\tau^4+\left(\tau\left(-\tau^3+\tau+3\right)+2\right)\tau\ln(\tau)+2\tau^2+\ln(\tau)\right) \\
&-(\tau-1)^2(\tau+1)^3\ln^2(\tau+1)+2(\tau-1)(\tau+1)^2\left(\tau+(\tau+1)^2\ln(\tau)\right)\ln(\tau+1)] \\
&+\pi^2(3\tau(\tau(\tau(15\tau+14)-3)-12)-6)\Bigg\},
\end{aligned}
$$

$R\gamma \to c\bar{c}\left[{}^1S_0^{[8]}\right]$ @ 1 loop, cross-check

In the combination of 1-loop results in the EFT:

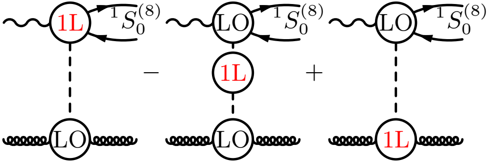

the $\ln r$ cancels and it should reproduce the the Regge limit$(s \gg -t)$ of the *real part* of the $2 \to 2$ 1-loop QCD amplitude:

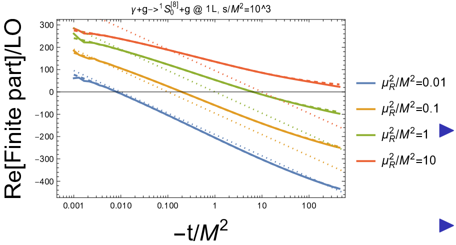

Solid lines – QCD, dashed lines – EFT, dotted lines – $-2C_A \ln(-t/\mu_R^2)\ln(s/M^2)$

$$\gamma + g \to c\bar{c}\left[{}^1S_0^{(8)}\right] + g.$$

- The $2 \to 2$ QCD 1-loop amplitude can be computed numerically using `FormCalc` (with some tricks, due to Coulomb divergence)
- The Regge limit of $1/\epsilon$ divergent part agrees with the EFT result
- For the finite part agreement within few % is reached, need to push to higher s

μ_F-variation

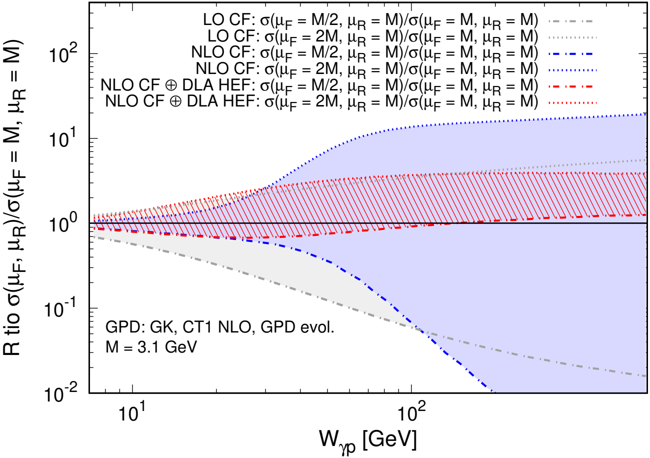

μ_R-variation

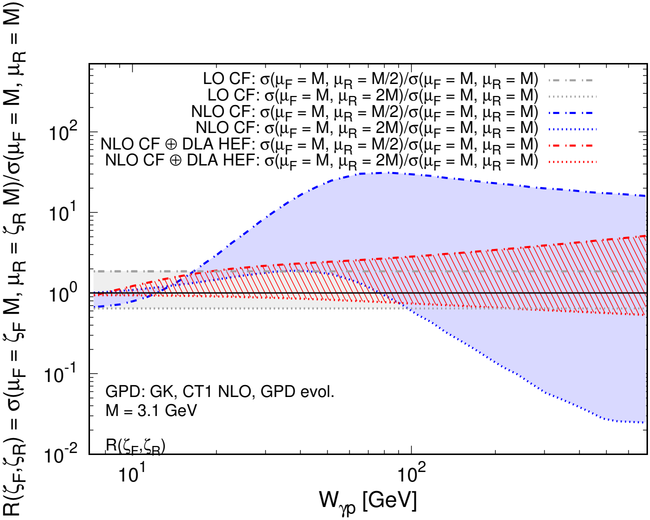

The increase of μ_R-variation of the matched result with energy is due to the μ_R-dependence of the $C_i^{(\text{HEF})}(\rho) \sim \rho^{-\hat{\alpha}_s(\mu_R)}$ for $\rho \to 0$.

Backup: DGLAP P_{gg} at small z

LO: $P_{gg}(z) = \frac{2C_A}{z} + \ldots \Leftrightarrow \gamma_N = \frac{\hat{\alpha}_s}{N}$

Plot from hep-ph/1607.02153 with my curve (in red) for the **strict LLA:**

$\frac{\hat{\alpha}_s}{N}\chi_{LO}(\gamma_{gg}(N)) = 1 \Rightarrow \gamma_{gg}(N) = \frac{\hat{\alpha}_s}{N} + 2\zeta(3)\frac{\hat{\alpha}_s^4}{N^4} + 2\zeta(5)\frac{\hat{\alpha}_s^6}{N^6} + \ldots$

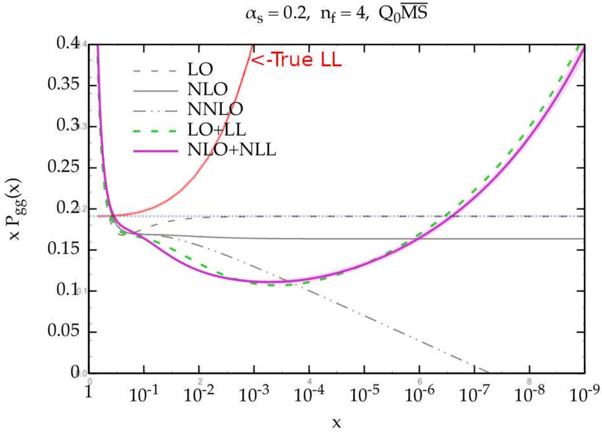

The “LO+LL” and “NLO+NLL” curves represent a form of matching between DGLAP and BFKL expansions, in a scheme by Altarelli, Ball and Forte which is more complicated than the **strict LL or NLL approximation**.

Effect of anomalous dimension beyond LO

Effect of taking **full LLA** for $\gamma_{gg}(N) = \frac{\hat{\alpha}_s}{N} + 2\zeta(3)\frac{\hat{\alpha}_s^4}{N^4} + 2\zeta(5)\frac{\hat{\alpha}_s^6}{N^6} + \ldots$ together with NLO PDF.

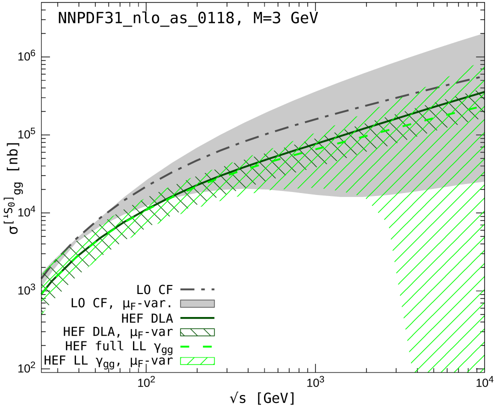

Scale-fixing solution

Studied in [Lansberg, Ozcelik, 20'], [Lansberg *et.al*, 21']. For J/ψ **photoproduction**:

$$\frac{d\sigma_{\gamma p}^{(\mathrm{LO+NLO})}}{d\ln\mu_F^2} \propto \left(\frac{\alpha_s}{2\pi}\right)^2 \int\limits_0^{\eta_{\max}} d\eta \left\{ \ln(1+\eta)\left[c_1(\eta\to\infty) + \bar{c}_1(\eta\to\infty)\ln\frac{M^2}{\mu_F^2}\right] \right.$$
$$\left. \times \left(f_g(x_\eta,\mu_F^2) + \frac{C_F}{C_A} f_q(x_\eta,\mu_F^2)\right) + \text{non-singular terms at } \eta \gg 1 \right\}$$

"principle of minimal scale-sensitivity" $\Rightarrow$ for J/ψ **photoproduction**:

$$\hat{\mu}_F = M \exp\left[\frac{c_1(\eta\to\infty)}{2\bar{c}_1(\eta\to\infty)}\right] \simeq 0.87M,$$

for η_c-hadroproduction:

$$\hat{\mu}_F = M \exp\left[\frac{A_1}{2}\right] = \frac{M}{\sqrt{e}} \simeq 0.61M.$$

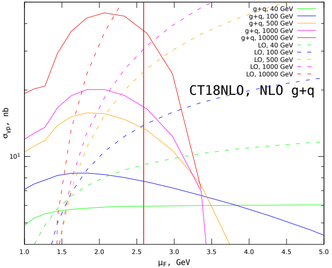

The $\hat{\mu}_F$-scale removes corrections $\propto \alpha_s^n \ln^{n-1}(1+\eta)$ from $\hat{\sigma}_i(\eta)$ and resums them into PDFs. But is such resummation complete?